

10-20-2005

# Development of Laser System to Measure Pavement Rutting

Hongzhi Wang  
*University of South Florida*

Follow this and additional works at: <https://scholarcommons.usf.edu/etd>

 Part of the [American Studies Commons](#)

---

## Scholar Commons Citation

Wang, Hongzhi, "Development of Laser System to Measure Pavement Rutting" (2005). *Graduate Theses and Dissertations*.  
<https://scholarcommons.usf.edu/etd/903>

This Thesis is brought to you for free and open access by the Graduate School at Scholar Commons. It has been accepted for inclusion in Graduate Theses and Dissertations by an authorized administrator of Scholar Commons. For more information, please contact [scholarcommons@usf.edu](mailto:scholarcommons@usf.edu).

Development of Laser System to Measure Pavement Rutting

by

Hongzhi Wang

A thesis submitted in partial fulfillment  
of the requirements for the degree of  
Master of Science in Civil Engineering  
Department of Civil and Environmental Engineering  
College of Engineering  
University of South Florida

Major Professor: Jian Lu, Ph.D.  
Ram Pendyala, Ph.D.  
Elaine Chang, Ph.D.

Date of Approval:  
October 20, 2005

Keywords: Camera, Scanner, Sensor, Transverse Profile, Vehicles

© Copyright 2005, Hongzhi Wang

## **DEDICATION**

This work is dedicated to my wife Rui Cheng and our incoming first-born baby.

## **ACKNOWLEDGEMENTS**

The author of the thesis would like to thank Dr. Lu for his supervision of the thesis and consistent guidance and support during the whole process of pursuing the master's degree in civil engineering. Thanks also go to Drs. Pendyala and Chang for their assistance and willingness to serve as the committee members.

## TABLE OF CONTENTS

LIST OF TABLES	iv
LIST OF FIGURES	v
ABSTRACT	ix
CHAPTER 1 INTRODUCTION	1
1.1 Introduction and Background	1
1.2 Statement of the Problem	3
1.3 Purposes of the Project	4
1.4 Organization of the Study	4
CHAPTER 2 REVIEW OF THE LITERATURE	5
2.1 Chapter Overview	5
2.2 Traditional Ways to Measure the Rut Depth	5
2.3 Methods of Automated Technologies	8
2.3.1 Ultrasonics	10
2.3.2 Point Lasers	13
2.3.3 Optical	16
2.3.4 Scanning Lasers	22
2.4 Chapter Summary	25
CHAPTER 3 SYSTEM DEVELOPMENT	27
3.1 System Requirements	27
3.1.1 Commercially Available Scanners	27

3.1.2 AR4000 Laser Scanner	28
3.2 System Improvements	33
3.3 System Testing	35
3.4 Software Development	37
CHAPTER 4 METHODOLOGY	40
4.1 Calibration	40
4.2 Analytical Process	44
4.2.1 Straight-Edge Algorithm	45
4.2.2 Wire Model Algorithm	47
4.2.3 Pseudo-Rut Algorithm	48
4.3 Straight-Edge Model and Algorithm for the Study	49
CHAPTER 5 DATA COLLECTION AND DATA ANALYSIS	52
5.1 Data Collection	52
5.2 Data Analysis	53
5.2.1 Data Sheet	53
5.2.2 Initial Angles	54
5.2.3 Scope Line	55
5.2.4 Moving Average	57
5.2.5 Analytical Process	58
5.2.6 Repeatability and Correlation	59
5.2.6.1 Repeatability	59
5.2.6.2 Correlation	60

CHAPTER 6 SUMMARY, CONCLUSIONS AND RECOMMENDATIONS	68
6.1 Summary	68
6.2 Conclusions	70
6.3 Recommendations	71
REFERENCES	72

## LIST OF TABLES

Table 3.1 Comparison of Commercially Available Scanning Laser Rangefinders	27
Table 4.1 Summary Output of Linear Regression	42
Table 4.2 ANOVA of Liner Regression	42
Table 5.1 Comparison of Real Rut Depth with 10 Values Obtained by the Scanner	67



## LIST OF FIGURES

Figure 1.1	FDOT Pavement Condition Forecast	2
Figure 1.2	The Demonstration of a Rut	3
Figure 2.1	Formation of the Pavement Rutting	6
Figure 2.2	RAMM Rut Depth Rating	7
Figure 2.3	Demonstration of Manual Measurement of Rut Depth	8
Figure 2.4	FDOT Survey Vehicle	9
Figure 2.5	The ROMDAS TPL Vehicle	10
Figure 2.6	Illustration of Fire Sequence of ROMDAS TPL	12
Figure 2.7	The Transverse Profile of Firing	13
Figure 2.8	The Demonstration of 3 Laser Points	13
Figure 2.9	DCV Laser Configuration	14
Figure 2.10	The Demonstration of 13 Laser Points	15
Figure 2.11	The RoadSTAR Transverse Evenness Measuring Device	15
Figure 2.12	A Fan-Shaped Measuring Beam with 23 Sensors	16
Figure 2.13	The Optical Method on Transverse Profile	17
Figure 2.14	Working Mechanisms	18
Figure 2.15	Optical Laser Scanner	18
Figure 2.16	Installation of Optical Laser Scanner	19
Figure 2.17	Laser Line by Camera	19
Figure 2.18	Height Profile in Real Time	19

Figure 2.19 INO Rut System	21
Figure 2.20 The Vehicle with INO Rut System	21
Figure 2.21 Model with One Laser Scanner	22
Figure 2.22 The Vehicle with Laser Scanner	22
Figure 2.23 Working Mechanisms of Mandli's Pavement Profile Scanner (PPS)	23
Figure 2.24 Scanning Orientation of PPS	23
Figure 2.25 Scanning Applications by Laser Scanners in Different Countries	24
Figure 2.26 Various Application of Laser Scanners on Vehicles	25
Figure 2.27 Impact of the Different Lateral Placement on Rut Depth	26
Figure 3.1 The Mechanism of the Rangefinder	29
Figure 3.2 AR4000-LIR Rangefinder	30
Figure 3.3 AccuRange Line Scanner	31
Figure 3.4 Laser Scanner with the Mirror	32
Figure 3.5 The Developed Scanner	33
Figure 3.6 The Exterior Appearance of Improved Scanner	34
Figure 3.7 The Interior Appearance of Improved Scanner	34
Figure 3.8 The Working Mechanism of the Laser Scanner	35
Figure 3.9 Installation of the Frame and the Scanner	36
Figure 3.10 On Site Measurement	36
Figure 3.11 Interface of Data Collection Software	37
Figure 3.12 Interface of Data Sheet (1)	38
Figure 3.13 Interface of Data Sheet (2)	39
Figure 4.1 Demonstration of Factory Calibration	40

Figure 4.2	Standard Plane	40
Figure 4.3	Results of Floor Calibration	41
Figure 4.4	The Curve of Linear Regression	42
Figure 4.5	The Scanning Results with 2 Layered Boards	43
Figure 4.6	The Moving Averages of the Two Layered Boards	44
Figure 4.7	Example of Straight-Edge Simulation	45
Figure 4.8	Example of Calculating Rut Depth	46
Figure 4.9	Example of Wire Model	48
Figure 4.10	Definition of Pseudo-Ruts	48
Figure 4.11	Implications of Slope Normalization on Pseudo-Ruts	49
Figure 4.12	Picture of Using Straight-Edge Method for Rut Depth	50
Figure 4.13	Implications of Straight-Edge Datum	51
Figure 5.1	Sample Data Sheet	54
Figure 5.2	The Mechanism of Initial Angles	55
Figure 5.3	The Data Discretion in the Dark Pavement	56
Figure 5.4	A Closer Look of the Data Discretion	56
Figure 5.5	The Comparison between the Original Ling and the Scope Line	57
Figure 5.6	The Results of Rut Depth Measurement	59
Figure 5.7	The Results of Repeatability Tests	60
Figure 5.8	The Manual Measurement of the Left Rut Depth	61
Figure 5.9	The Manual Measurement of the Right Rut Depth	61
Figure 5.10	On Site Rut Measurement Test 1	62
Figure 5.11	On Site Rut Measurement Test 2	62

Figure 5.12 On Site Rut Measurement Test 3	63
Figure 5.13 On Site Rut Measurement Test 4	63
Figure 5.14 On Site Rut Measurement Test 5	64
Figure 5.15 On Site Rut Measurement Test 6	64
Figure 5.16 On Site Rut Measurement Test 7	65
Figure 5.17 On Site Rut Measurement Test 8	65
Figure 5.18 On Site Rut Measurement Test 9	66
Figure 5.19 On Site Rut Measurement Test 10	66

# **DEVELOPMENT OF LASER SYSTEM TO MEASURE PAVEMENT RUTTING**

**Hongzhi Wang**

## **ABSTRACT**

Asphalt pavement rutting is one of the most common and destructive pavement distresses observed on U.S. roads, particularly in the urban environment at intersections. They are an important indicator of the structural integrity of the pavement as well as having an impact on road user safety. For these reasons, most road agencies regularly monitor the levels of rut depths on their pavement. There are four technologies used for estimating rut depth in automated measurement way: ultrasonics, point lasers, scanning lasers, Optical.

This thesis will focus on the development of the laser scanner rut depth measurement system, including the improvement of the hardware design, the software development and data analysis.

In order to evaluate the accuracy and correction of the laser scanner system, the researcher used it to measure different pavement in different situations. This research focused on the performance measures, such as correlativity, repeatability.

From field experiments and data analysis, the following results had been obtained:

1. Laser scanner showed satisfactory repeatability performances;
2. Laser scanner has good correlations with manual rut data.

3. High power laser scanner in dark asphalt has good correlations with in light pavement.

The findings of this research will contribute to the development of laser system in the measurement of pavement rutting.

## CHAPTER 1

### INTRODUCTION

#### 1.1 Introduction and Background

There are five major asphalt pavement distresses that may result in loss of performance: fatigue cracking; rutting; thermal cracking; friction; and moisture susceptibility. Asphalt pavement rutting is one of the most common and destructive pavement distresses observed on U.S. roads, particularly in the urban environment at intersections.

Pavement rutting is a critical distress in flexible pavements because rutted pavements pose a serious safety hazard. During wet weather, water tends to collect in the pavement ruts, increasing the potential for hydroplaning and associated wet-weather accidents. Pavement rutting also may have a detrimental effect on overall ride quality and, hence, user satisfaction.

It is an important indicator of the structural integrity of the pavement as well as having an impact on road user safety. For these reasons, most road agencies regularly monitor the levels of rut depths on their pavement.

Florida Department of Transportation measures the rutting and cracking of most state roads every year in order to forecast the pavement condition (figure 1.1). They then can decide which roads need maintenances in the following year.

# FLORIDA DEPARTMENT OF TRANSPORTATION

5

## ALL SYSTEM PAVEMENT CONDITION FORECAST

PAVEMENT IMPROVEMENT PROJECTS IN FM WPA TENTATIVE PLAN -- 2005 - 2010, EXTRACTED ON 03/10/2005

SORT BY RDWYID MILEPOST R ASCENDING L DESCENDING 10:53 Thursday, March 10, 2005

----- DISTRICT = 7 COUNTY = HILLSBOROUGH -----

RDWYID	EMP	EMP RW	SYS	TYP	SPD	DISTRESS	SURVEYED YEAR												FUTURE		
SR	US	G_EMP	G_EMP LN	%T	ADPT	RATINGS	1980	1981	1982	1983	1984	1985	1986	1987	1988	1989	1990	1991	1992		
INTERSECT AT (MP SIDE)							SURFTYPE =====														
ITMSEG-P W_EMP W_EMP RW FY-P WMMX-F																					
CONTRACTOR (AGE ONE YEAR) PASTYPE							1993	1994	1995	1996	1997	1998	1999	2000	2001	2002	2003	2004	2005	2010	
ITMSEG-F W_EMP W_EMP RW FY-F WMMX-F							(REG)														
10020000	0.325	2.961	C	1	1	40	CRACKING	3.4*	10.0	10.0			8.7	8.7	8.7	8.7	8.7	10.0	7.5		
685	41		3	5.0	10500	RIDE	4.0*	6.3*	5.4*				6.1*	6.2*	6.2*	6.0*	5.3*	5.6*	6.0*		
TYLER ST E * ( 0.3C) FC3 RUTTING							2.0*	10.0	10.0				9.0	9.0	9.0	9.0	9.0	9.0	7.0		
2555071	0.000	2.961	C	2000	0012	CRACKING	7.5	7.5	7.5	7.5	7.5	7.5	6.5	5.5*		10.0	10.0	10.0	10.0	10.0	
APAC-FLORIDA INC (2002) S RIDE							5.7*	5.8*	5.3*	4.9*	5.4*	5.5*	0.8*	4.5*		8.1	7.5	7.5	7.1	5.6	
							RUTTING	7.0	8.0	7.0	7.0	7.0	7.0	7.0	7.0		9.0	7.0	8.0	8.0	7.0
10020000	2.961	4.335	C	1	1	40	CRACKING	2.7*	10.0	10.0			8.7	8.7	8.7	8.7	7.0	9.0	9.0		
685	41		4	5.0	19400	RIDE	0.5*	6.3*	6.5				6.1*	6.0*	6.5	6.3*	5.6*	5.8*	6.4*		
E VIOLET ST ( 3.0C) FC3 RUTTING							2.0*	10.0	10.0				9.0	9.0	8.0	7.0	7.0	7.0	7.0		
2555461	2.491	4.368	C	1996	0213	CRACKING	9.0	7.5	7.5	7.5	10.0	10.0	10.0	10.0	10.0	9.5	9.5	9.5	9.0	8.5	
OHM REMEDIATION SERVICES (1997) S RIDE							5.1*	5.3*	5.1*	4.7*	7.5	8.0	6.7	6.2*	6.1*	7.0	6.6	7.1	6.5	5.9	
							RUTTING	7.0	7.0	7.0	6.0*	10.0	9.0	10.0	10.0	10.0	10.0	10.0	9.0	9.0	
10020000	4.335	5.100	C	1	1	40	CRACKING	3.7*	3.7*	7.7			8.7	8.7	9.4	10.0	10.0	10.0	10.0		
685	41		4	3.9	21000	RIDE	6.5	5.2*	4.9*				6.1*	3.8*	7.8	7.6	7.6	7.4	7.5		
SLIGH AVE W ( 4.4L) FC3 RUTTING							8.0	4.0*	5.0*				6.0*	6.0*	6.0*	8.0	8.0	8.0	8.0		
2557801	2.961	5.355	C	1995	0220	CRACKING	10.0	10.0	10.0	10.0	10.0	10.0	10.0	10.0	10.0	10.0	10.0	10.0	10.0	10.0	
J W CONNER & SONS INC (1997) S RIDE							7.3	7.4	7.2	6.7	8.1	8.8	8.6	8.8	8.6	8.6	7.9	7.7	7.3	7.1	
							RUTTING	9.0	8.0	8.0	8.0	10.0	10.0	10.0	10.0	10.0	10.0	10.0	9.0	9.0	9.0

Figure 1.1 FDOT Pavement Condition Forecast

Ruts seem pretty straight forward, that is to say, it is easy to tell when you're in a rut (figure 1.2). But it is not as easy to determine when a groove in pavement is a rut. It is hard to define a rut precisely.

Rutting of pavements can represent a major hazard to users as well as being an early indicator of pavement failure. Rut depth measurements are therefore usually included in most road monitoring programs.





Figure 1.2 The Demonstration of a Rut

Traditionally, rut depths were measured manually using a straight-edge and wedge. While simple to execute, this method resulted in irregular measurements at wide intervals as it was usually impractical to sample an entire network manually. The advent of non-contact measurements using ultrasonics and lasers has rendered the manual method obsolete in many countries. These methods consist of measuring the transverse profile of the pavement and then analyzing the data to calculate the rut depth under a simulated straight-edge.

### **1.2 Statement of the Problem**

The examination of the current literature in rut depth and pavement provides insight into several major issues faced by researchers. The first challenge is that traditional methods to measure rut depth are hardly to provide accurate information and difficult to be applied in the large scale measurement. The updated methods with the involvement of camera and laser scanners are out of reach of general users because of their high costs. There is little information on an affordable way to measure the rut depth with relatively high accuracy. All of these issues need to be addressed by the

transportation researchers and a reasonable solution is needed for the both research purposes and commercial purposes.

### **1.3 Purpose of the Project**

The purpose of the project is to explore the possibility of using AR4000 as an affordable and accurate laser scanner to measure the rut depth. Comparing to the traditional ways of manual measurement, AR4000 is more advanced in the regard that it uses laser scanner and can reach the accuracy and extend the scope of measurement easily. On the other hand, AR4000 is more affordable compared with other laser scanners and optical devices. In this thesis, the rationale of choosing AR4000 will be described based on the review of the literature. The detailed description of the application and quality of work by using AR4000 will be reported, and thus, the advantage of AR4000 laser scanner will be obvious by the end of the thesis.

### **1.4 Organization of the Study**

The remaining chapters of this proposal cover relevant literature, research methodology utilized in this research, and results of the projects. Chapter two reviews literature pertaining to rut depth and both traditional and more current methods applied for the measurement. This chapter also serves as the basis for the study. Chapter three contains a detailed description of the methods of research used in the study. This includes the installation of both hardware and software, how data will be collected, as well as a detailed overview of the data analysis. Chapter four concludes the study by reporting the results of the measurement by the devices selected by the researcher and by recommending for future research directions.

## CHAPTER 2

### REVIEW OF THE LITERATURE

#### 2.1 Chapter Overview

This chapter reviews the related literature. The chapter begins by the introduction of traditional ways to measure the rut depth, followed by more current methods. The author compared and contrasted several methods by using different laser scanners to measure the rut depth. The advantages and disadvantages of each type were revealed. At the end of the chapter, the author introduced the rationale of selecting AR 4000 laser scanner to measure rut depth, the specifications and its functionality.

#### 2.2 Traditional Ways to Measure the Rut Depth

Generally, to be considered a rut, a depression must be continuous, but exactly how deep and how long the depression must be before it is technically or legally defined as a rut has not been satisfactorily determined because no one has been able to accurately measure pavement surfaces.

Ruts occur when traffic loading displaces the bituminous material that makes up part of the pavement structure (figure 2.1). How the material is displaced depends on the composition of the pavement. It's either displaced laterally from the wheel tracks toward the shoulder and centerline and between the wheel tracks, or vertically.

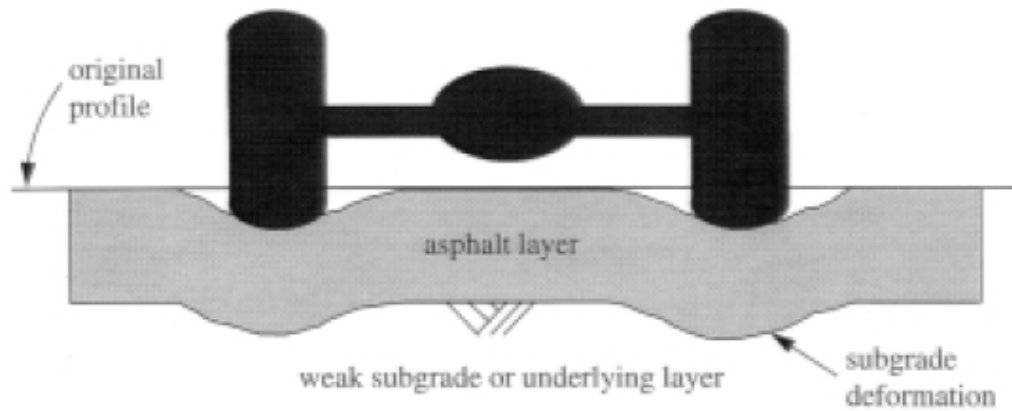


Figure 2.1 Formation of the Pavement Rutting

Rutting is a problem because water collects in the ruts and subjects the pavement to ponding and freezing, eventually causing the pavement to deteriorate. Ponding in ruts also creates possible hazards for drivers, but the wheel tracks themselves can also pose problems. If the depression is deep enough, the vehicle rides in a trough. As long as the vehicle stays in the trough, the rut poses no problem. However, when a vehicle goes to moves out of the trough it could become unstable.

Different vehicles respond in different ways to the same rut, depending on the size of the vehicle, its wheel base, and the design and condition of its tires. Current knowledge of how these variables interact is insufficient to predict how different vehicles will respond to the same road condition. In other words, it is unclear at what point a rut becomes a problem.

Improvements in measuring pavement surface are expected to provide a better understanding of the role pavement rutting plays in vehicle response.

Regular data collection is essential for the proper monitoring of road condition, and thus the asset value. Accordingly, many road controlling authorities have annual data

collection programs. One of the data collection methods is to collect manual data.

This is a visual assessment of the pavement condition collected in accordance with the RAMM Rating Guide (Transfund, 1997). The pavement distresses are recorded along a 'Rating Length'.

As illustrated Figure 2.2, rutting in RAMM is defined as the length of individual wheel path in meter where rutting (wheel tracking) exceeds 30 mm in depth measured from a 2 meter straight-edge laid transversely across the wheel path. Only the length exceeding 30 mm is measured. Since there are 4 x 50 meter lengths over a 50 meter rating section, there is a maximum possible value of 200 meter for this measure.

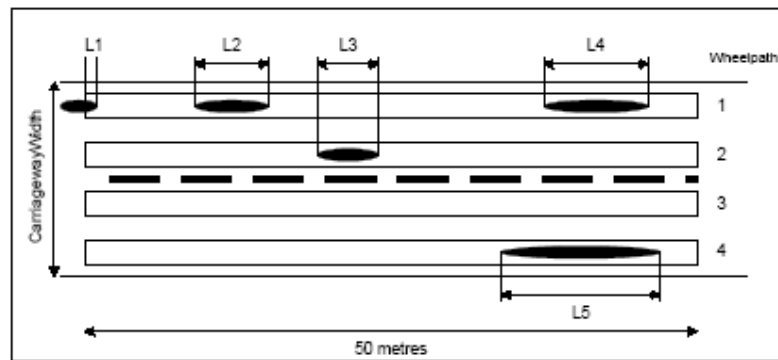


Figure 2.2 RAMM Rut Depth Rating

With the implementation of predictive modeling for pavement deterioration, there has been a shift of emphasis away from the RAMM approach of the length of pavement with rut depths greater than 20/30 mm to the use of the mean rut depth. This trend is likely to continue as it is consistent with the output from the predictive modeling.

Until recently, pavement rutting was measured the old fashioned way with a ruler and either a straight edge or a wire. These methods do not lead to accurate results in a

large scale measurement. The depth of a rut can vary depending upon the length of the straight edge used. Using a wire in place of a straight edge compensates for the curvature of the road surface, but is still a slow tedious process: two people secure the ends of the wire stretching from the centerline to the shoulder by stepping on it while a third person measures the depression, if any, from the wire to the bottom of a rut. In either case, crews typically record two or three such samplings per mile, so the compiled rut profile is sketchy at best. To make matters worse, traffic must be routed around the lane being measured.



Figure 2.3 Demonstration of Manual Measurement of Rut Depth

### 2.3 Methods of Automated Technologies

Besides manual data collection, another method that is widely used is to collect automated data. By applying this method, roughness is collected either using a laser profilometer or a response-type meter (e.g. NAASRA meter). State Highways are

only measured with profilometers while response-type meters or profilometers are used for local authorities. Rut depths are collected with lasers or ultrasonics. Texture is collected with lasers, although mainly on State Highways. International Cybernetics Corporation (ICC) in Largo, Florida manufactured the FDOT Survey Vehicle (figure 2.4).



Figure 2.4 FDOT Survey Vehicle

The importance of timely corrective action for rutted pavements, coupled with the need for safe and efficient data collection, has led many State highway agencies to use automated survey vehicles to collect the data needed to assess and monitor the extent and severity of pavement rutting. Typically, these devices measure the distance from a reference point on the survey vehicle to the pavement surface at three or five points across the pavement width. These data are then used to compute an estimate of the depth of pavement rutting.

Automated measurements are made using lasers or ultrasonic transducers to measure the transverse profile of a pavement as a vehicle travels over it at highway speeds. There are four technologies used for estimating rut depths:

### 2.3.1 Ultrasonics

Ultrasonic sensors are the lowest cost sensors and are used in systems like ROMDAS and ARAN. These have sensors at approximately 100 mm intervals which measure up to 3 m across the pavement. Due to the speed of ultrasonics these systems typically sample at 2.5 – 5 m along the road. Figure 2.4 is an example of the MWH 30 sensor ultrasonic profilometer.

The measurement of the transverse profile is done using a 'transverse profile logger' (TPL). The ROMDAS TPL (figure 2.5) consists of a 2 m main section and 2 'wings' which can be lowered to extend the coverage. The photo below is of a ROMDAS TPL on the ART Sdn. Bhd. vehicle from Malaysia. Here, the wings have been folded up.



Figure 2.5 The ROMDAS TPL Vehicle



In the photo it will be noted that there is a white cylinder above the TPL. This is the temperature correction sensor. It consists of a sensor firing at a fixed target. If the distance to this target changes because of temperature, altitude or humidity, all the other measurements need to be corrected by a similar amount. Thus, the corrections for ambient conditions are done automatically with ROMDAS.

The measurements are done using five ultrasonic sensors and their associated circuitry in an environmentally protected housing (called an ultrasonic measurement system array or UMSA). The sensors are spaced at 100 mm intervals and will measure the distance to pavement with an accuracy of  $\pm 1.0$  mm. The main section contains four UMSA while the wings each contain one UMSA. A total of 30 sensors are therefore available when the main section and both wings are being used.

The advantage of this configuration is that in the event of a sensor failing, they can be quickly replaced by removing the entire UMSA and replacing it with a spare. This avoids the need to interrupt the survey to return for repairs.

The TPL electronics are compact and a system of 6 UMSA fits into a small case. It is possible to purchase the electronics separately to the housing or to build your own housing from plans that we can supply.

To eliminate the possibility of any interference, the sensors are fired sequentially and then combined to establish the overall profile. This is illustrated in the figure (figure 2.6) below.

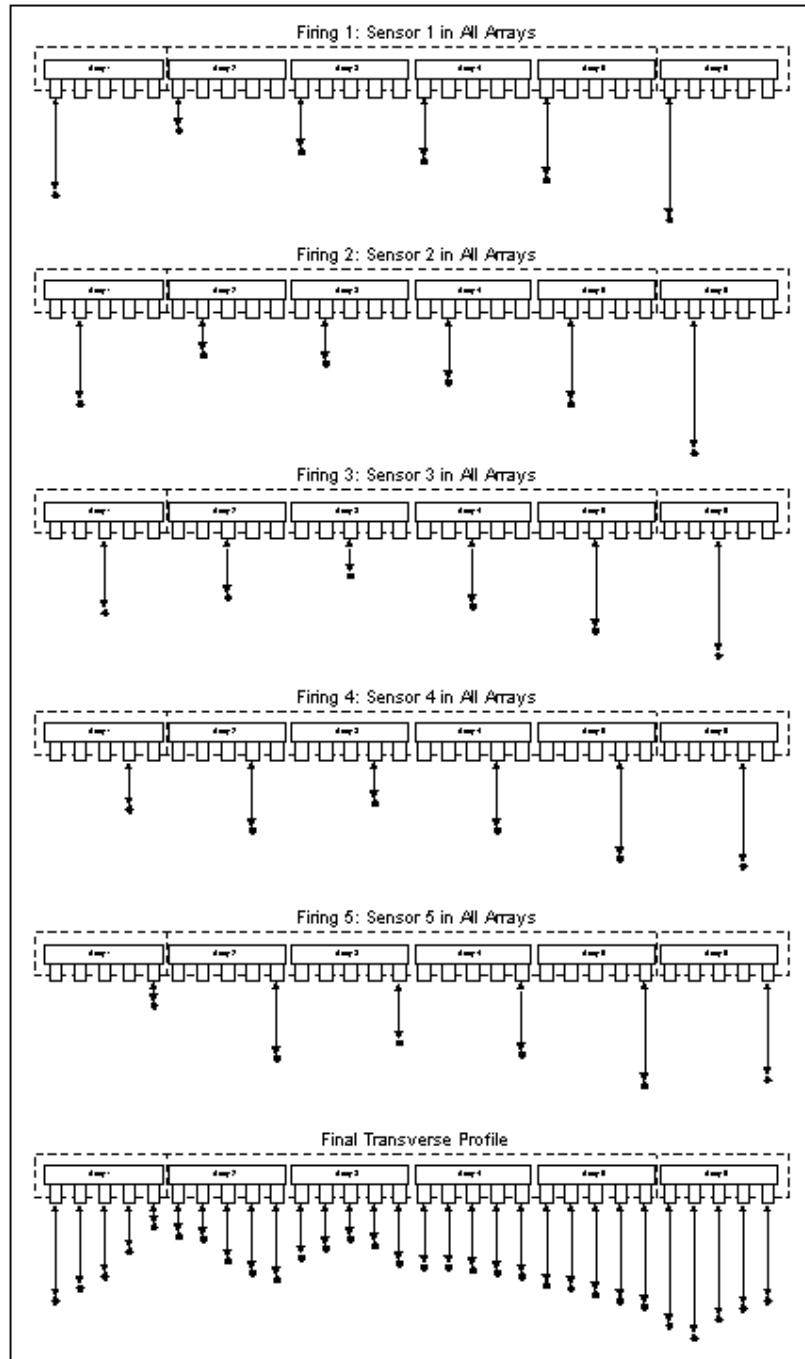


Figure 2.6 Illustration of Fire Sequence of ROMDAS TPL

The firing takes place over the space of about 1-2 m so the resulting transverse profile is not from the same point in space but is instead a composite formed from the five firings. This is illustrated below (figure 2.7). The firing of all sensors in all

UMSA takes approximately 0.125 s. The total longitudinal distance between sensors 1 and 5 in each array therefore depends upon the speed of the vehicle.

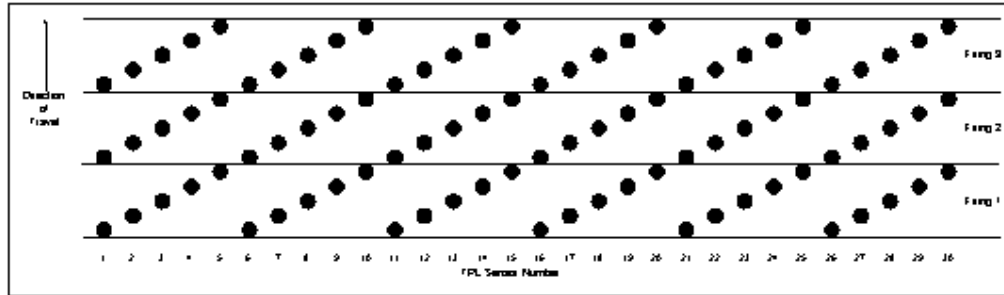


Figure 2.7 The Transverse Profile of Firing

### 2.3.2 Point Lasers

Point lasers give the elevation at a point. Simply using 3 point laser scanning, we can get the rut as illustrated in the following figure (Figure 2.7). Besides much faster than ultrasonics in the data collection, point lasers record the transverse profile at intervals as low as 10 mm along the road.

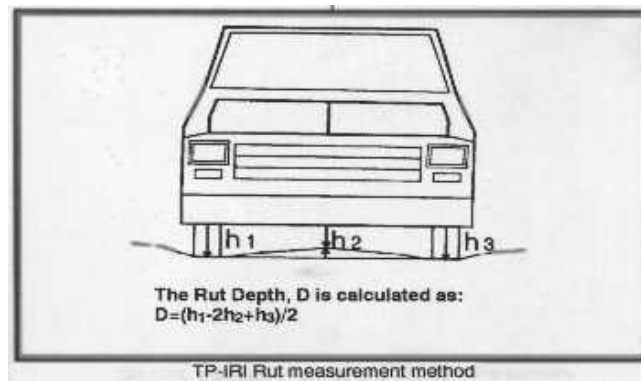


Figure 2.8 The Demonstration of 3 Laser Points

For more accuracy, Rutting in hot-mix asphalt (HMA) pavements is estimated using five lasers mounted in the front bumper of the DCV (figure 2.9). One sensor is located in the middle, one in each wheel path, and one on each side oriented at a 45° angle, as shown in Figure 2.8:

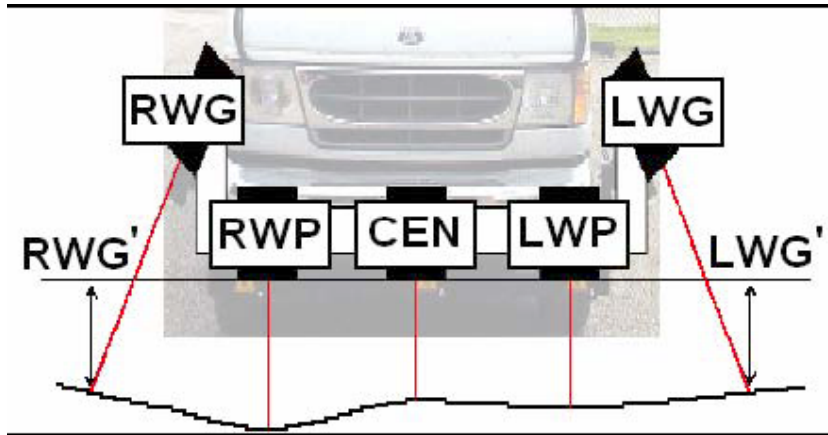


Figure 2.9 DCV Laser Configuration

Rut Depth Calculations are realized by the following formulas.

$$\text{Left Rut} = \text{LWP} - (\text{CEN} + \text{LWG}')/2$$

$$\text{Right Rut} = \text{RWP} - (\text{CEN} + \text{RWG}')/2$$

$$\text{Center Rut} = (\text{RWP} + \text{LWP})/2 - \text{CEN}$$

Rut depth is calculated where RWP, CEN, and LWP are the respective distances between the right wheel path, center, and left wheel path sensors and the pavement surface. The right wing (RWG) sensor and left wing (LWG) sensors are used to determine pavement surface heights (RWG' and LWG') at the edges of the test lane. The current 5-sensor configuration allows separate rut measurements for each wheel path. Before 2002, IDOT DCVs with a 3-sensor configuration provided only the estimated "center rut" by comparing the height at the center of the pavement with the average depth in the wheel paths. For the purpose of comparing current and historical data, the center rut measurement is stored in a pavement management database.

Recent Long Term Pavement Performance (LTPP) data analysis has provided information on the repeatability and accuracy of the rut statistics obtained with these devices.

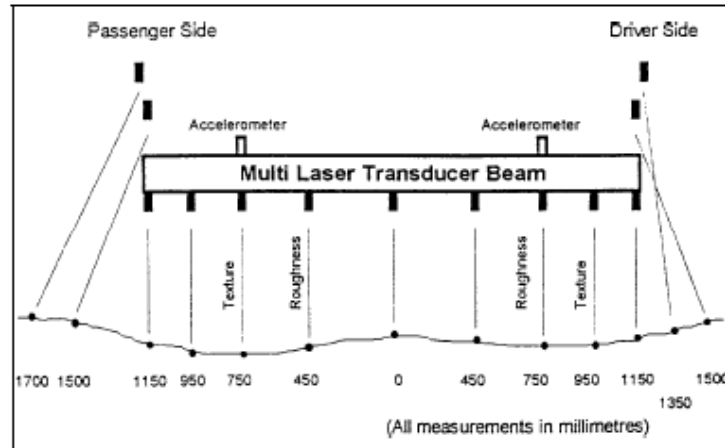


Figure 2.10 The Demonstration of 13 Laser Points



Figure 2.11 The RoadSTAR Transverse Evenness Measuring Device

The transverse evenness of the road is of major importance in terms of both road safety and driving comfort. Marked rutting may produce additional steering forces and lead to aquaplaning. The characteristic parameters of transverse evenness are rut

depth, profile depth and theoretical water film thickness in the right and left wheel tracks.

The RoadSTAR transverse evenness measuring device (figure 2.11) essentially consists of 23 laser sensors of laser class 3a with a measuring accuracy of 0.1 mm and a high-precision fiber gyroscope system for determining the crossfall of the road with a measuring accuracy of  $<0.1^\circ$ .

A measuring beam with a fan-shaped arrangement of 23 laser sensors (figure 2.12) is mounted to the front bumper of the vehicle. This configuration allows a lane width of 3.3 m to be measured with a design width of only 2.5 m. The spacing between measuring points of the transverse profile is 15 cm.

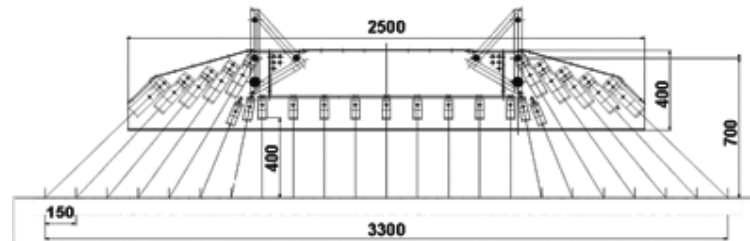


Figure 2.12 A Fan-Shaped Measuring Beam with 23 Sensors

### 2.3.3 Optical

Optical methods use digitized images of the transverse profile which are analyzed to estimate rut depths. These images may be produced using various photographic techniques, often supplemented by lasers.

The method used to acquire the rutting information is similar to a commonly used industrial process that measures 3D information. A flat plane of laser light is shone onto the road and a camera looks at the resultant line as shown in figure 2.13.

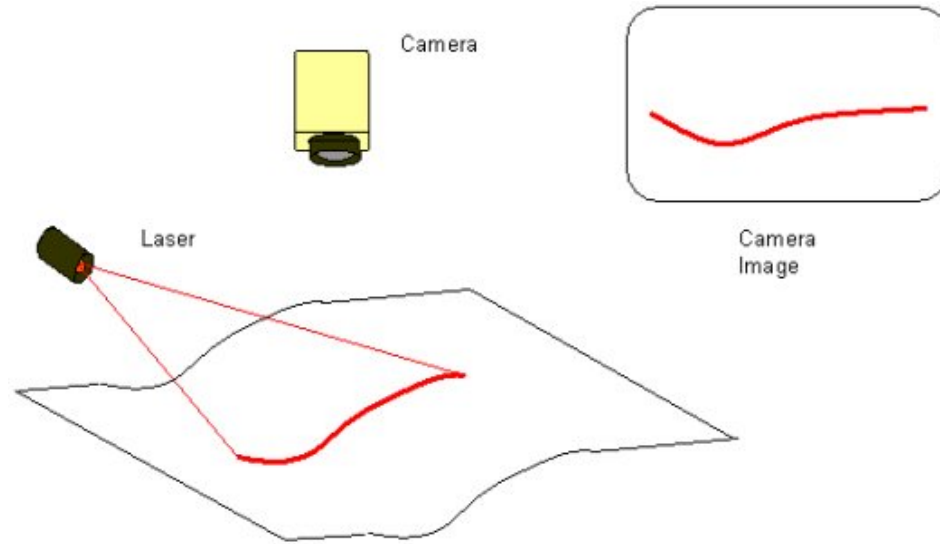


Figure 2.13 The Optical Method on Transverse Profile

The process of working is that the camera image is digitized; the line of light is recognized and recorded as raw data; the raw data is corrected to convert it into points in the real world; and the real world points are used to detect and measure ruts.

Both traditional and ultrasonic methods are relatively unaffected by normal environmental conditions. Excessive spray can reduce the accuracy of ultrasonic methods; however it does affect the optics of the camera. The cover of the topograph reduces spray but the optics has to be cleaned every so often. Sunlight has no effect on traditional methods but it can have a profound affect on the topograph. If too much sunlight gets in, it can reduce the effective measurement width. Most of the time the skirt on the topograph allows the full width to be measured but in practice, during heavy breaking down a hill or very uneven surfaces for example, the effective width will be diminished to 50% and very occasionally less.

Another theory that is widely used in the optical method of rut measurement uses the instantaneous profile laser scanner. This laser scanner is able to measure instantaneously the heights along a profile. A laser creates a bright line on the soil surface. A digital CCD camera looks at this line. The location of the laser line on the 2D CCD array depends on the height of the surface along the laser line (see figures below 2.14, 2.15 and 2.16). After calibration, the CCD coordinates (line, row) are converted to X and Z.

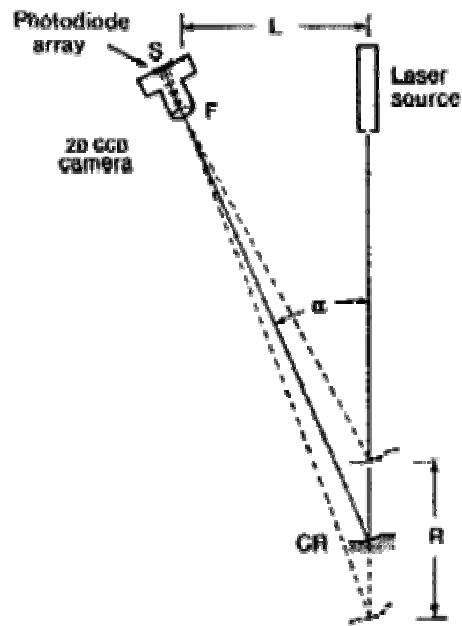


Figure 2.14 Working Mechanisms

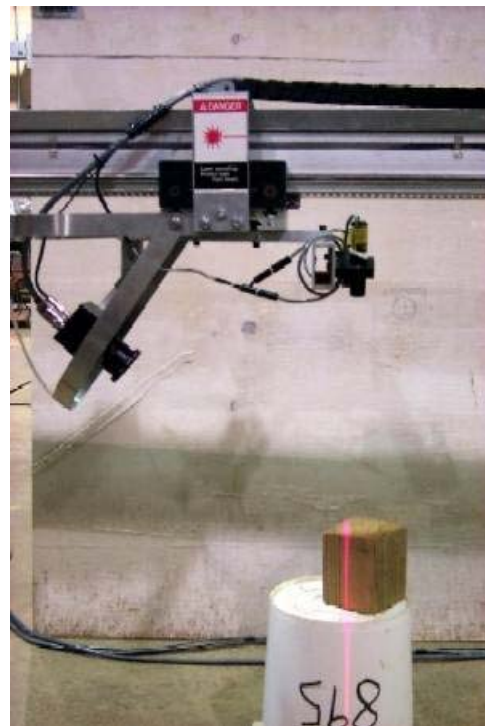


Figure 2.15 Optical Laser Scanner



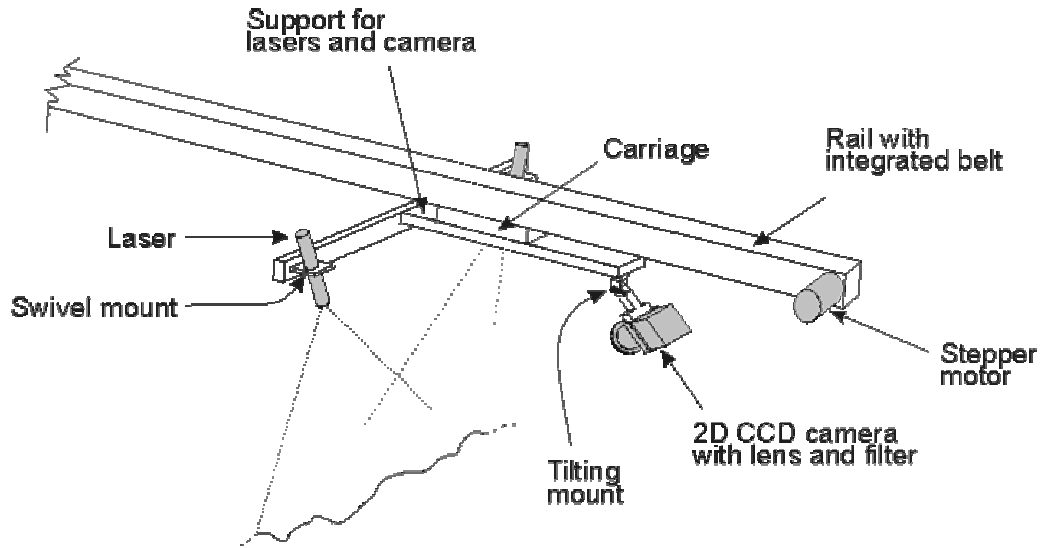


Figure 2.16 Installation of Optical Laser Scanner

The ensemble camera-laser is attached on a carriage. This carriage moves along a rail. A desktop PC pilots the carriage movement and the picture acquisition. The acquisition of successive height profiles is automatic. The pictures are processed in real-time (see figures below).

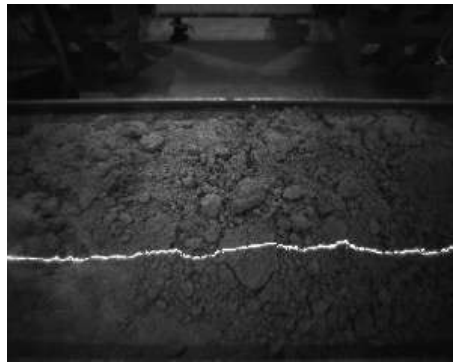


Figure 2.17 Laser Line by Camera

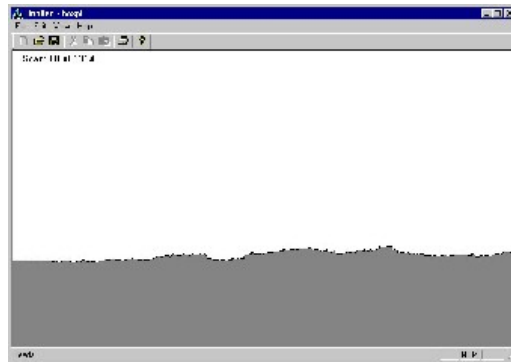


Figure 2.18 Height Profile in Real Time

The specification of the above described instantaneous profile laser scanner is described below: (Configured to measure soil surface roughness)

- One rail (no traversing frame)
- Resolution

- Along a profile: 0.5 mm
- Vertical resolution: 0.5 mm
- Distance between each profile: 0.5 mm
- Instantaneous profile length: 45 cm
- Scan distance: rail length (up to several meters!)
- 380 profiles / minute
- Indoor and outdoor uses

An example of such a system is the INO rut system which uses two lasers to project lines to the pavements and a special camera to measure deformations of the laser line.

INO has developed a 3D laser rut measurement system to detect and characterize pavement rutting. The system can acquire full 4 meter width profiles of a highway lane at inspection speeds of up to 100 km/h. It uses two laser profilers that acquire the shape of the pavement. Custom optics and high-power pulsed laser line sources allow the system to operate during the day or at night.

The system's maximum profile acquisition rate is 25 Hz. The system can continually monitor the vehicle's odometer to keep the longitudinal acquisition density constant, allowing the inspection vehicle to operate in normal traffic conditions. Road profile data is collected and processed in the vehicle and can then be compressed and stored with a GPS time stamp. Processing tasks include calibration and corrections due to the ride of the inspection vehicle.

Rut analysis algorithms have been developed to automatically measure short and wide radius ruts and rut depth.



Figure 2.19 INO Rut System



Figure 2.20 The Vehicle with INO Rut System

- Nb. of laser profilers: 2
- Sampling rate: up to 25 profiles/s
- Vehicle speed: 0 to 120 km/h
- Profile spacing: adjustable
- Transversal (width) resolution: 1280 points/profile
- Transversal field-of-view (nominal): 4 m
- Depth range of operation: 500 mm
- Depth accuracy:  $\pm 1$  mm
- Transversal (width) accuracy:  $\pm 3$  mm
- Laser profiler dimensions (approx.):  
140 mm(W) x 1052 mm(H) x 305 mm(D)
- Laser profiler weight: 22 kg

### 2.3.4 Scanning Lasers

This is a new technology not currently used in many parts of the world. These lasers measure what is almost a continuous profile. An example of such a system is the Phoenix Science 'Ladar' which samples a 3.5 m pavement width from a single scanning laser mounted 2.3 m above the ground. 950 points are sampled across the transverse profile, sampled every 25 mm along the pavement.

Mandli's Pavement Profile Scanner (PPS) system collects pavement testing data from a vehicle (figure 2.21 and 2.22) traveling at highway speeds using a phase measurement Laser Radar for unparalleled precision, range, and sample rate. The pavement scanner is mounted to the rear of the data collection vehicle with no hardware extending beyond the vehicle width. Full-lane transverse and longitudinal profiles can be collected safely and unobtrusively.

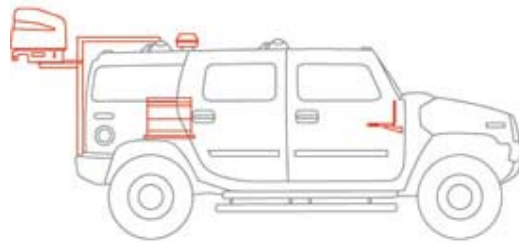


Figure 2.21 Model of One Laser Scanner      Figure 2.22 Vehicle with Laser Scanner

The core of the optical mechanical system is a rotating 6 sided polygon which synchronizes the modulated laser beam and receiver field-of-view as it sweeps the measurement spot through a  $90^\circ$  arc at a constant 1,000 times per second (figure 2.23). The resulting profile width is twice the height at which the polygon is mounted.

The design point is for a 4.3 meter profile, but this may be adjusted by moving the

scanner up or down. The separation between each new profile depends on the vehicle speed. For example, at 100 K.P.H. the profiles are separated by 2.8 mm.

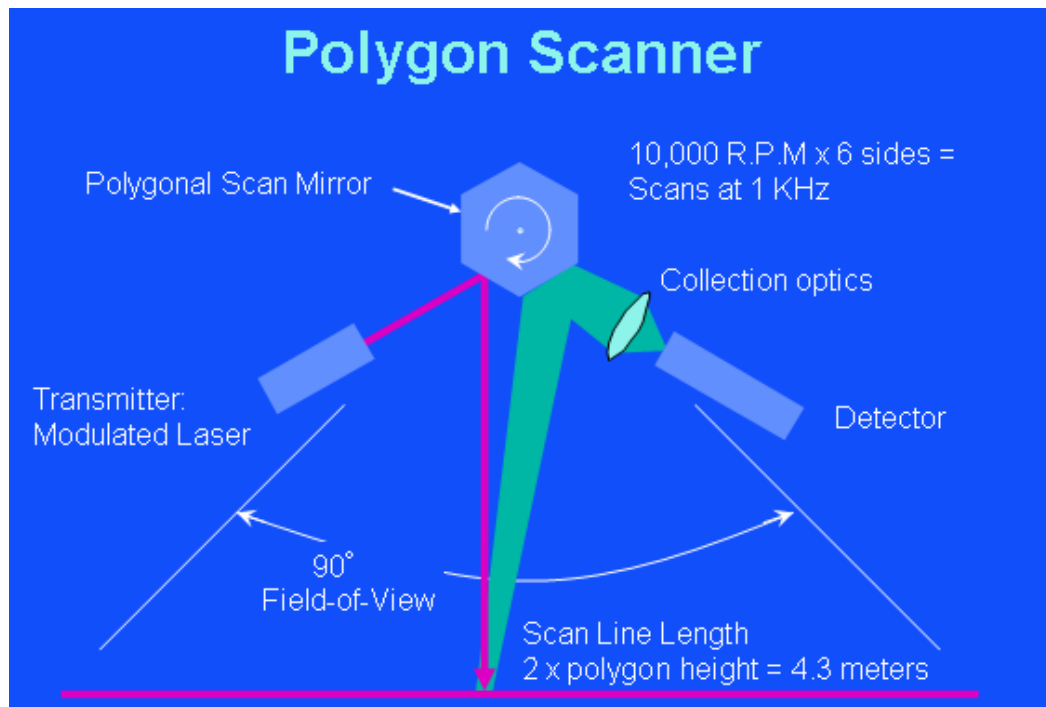


Figure 2.23 Working Mechanisms of Mandli's Pavement Profile Scanner (PPS)

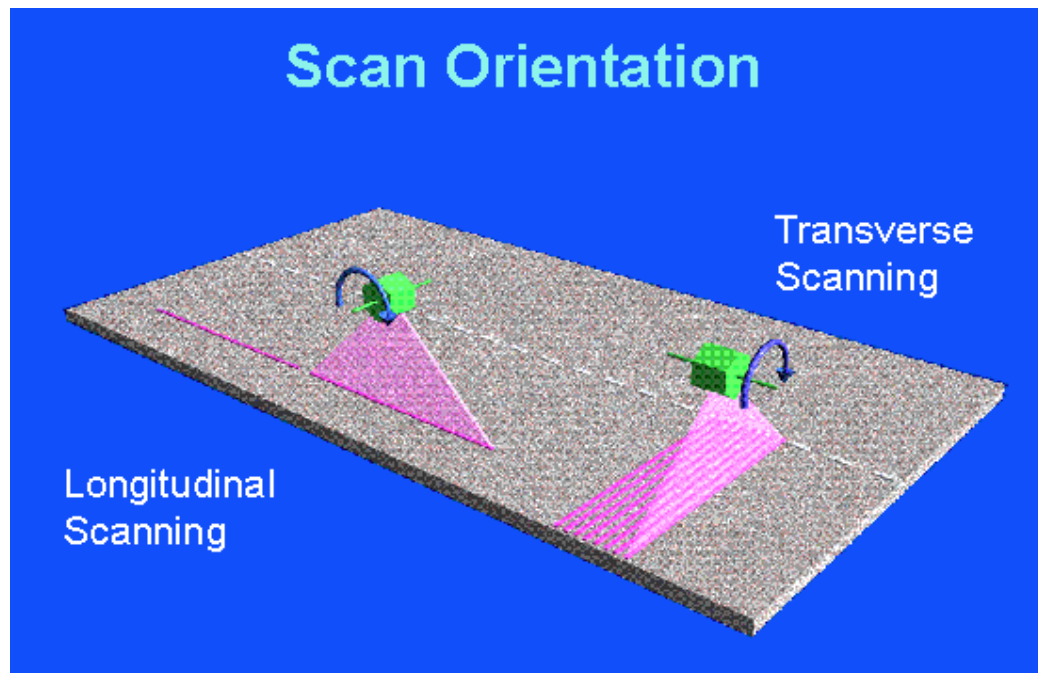


Figure 2.24 Scanning Orientation of PPS

The two primary ways to orient the scanner are orthogonal to the direction of travel of the test vehicle (figure 2.24). Longitudinal scanning was used for PSI's patented (in USA only) Rolling Wheel Deflection concept and has been shown to have potential for accurate longitudinal profile in stop-and-go traffic. Transverse scanning is the configuration used today for routine rut and ride quality measurements. Oblique scanning opens other unique possibilities, such as mapping the faulting at jointed PCC (white or concrete) pavements at numerous equally spaced transverse points across the pavement while still doing rut and ride. The applications will be illustrated in successive figure (figure 2.25 and 2.26).



Figure 2.25 Scanning Applications by Laser Scanners in Different Countries

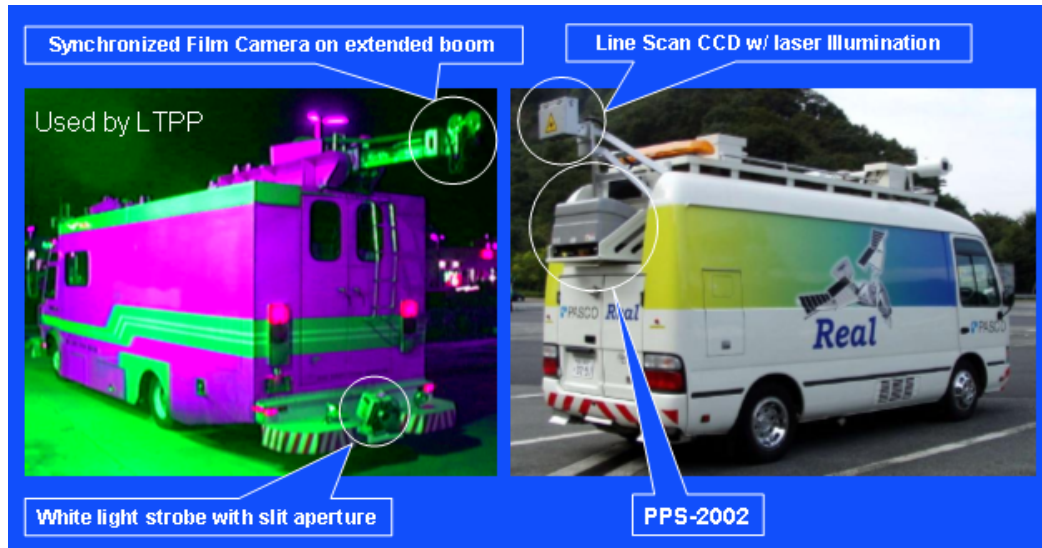


Figure 2.26 Various Application of Laser Scanners on Vehicles

Although this laser scanner can provide accurate information about the rut depth, it is very expensive. The whole system is more than \$300,000 (not including the vehicle and the computer).

## 2.4 Chapter Summary

In this chapter, the author reviewed the related literature in the measurement of rut depth. There are basically two methods for data collection in this field: manual data and automated data. The disadvantage for traditional way of data collection and analysis is very obvious, that is, it is hard to obtain accurate and adequate information by manual data collection. Among 4 basic ways of data collection within automated methods, the ultrasonics and laser points method are cheaper, yet in the context of rut depth measurements, the effects of sampling are exacerbated by lateral placement variations. This sees the operator not positioning the vehicle in exactly the same wheel track between successive surveys. While this is typically not a problem during equipment validation, where the vehicles are operated in a very controlled manner

over clearly marked wheel paths, it is an issue during operational surveys. The situation won't change much when the points are added from 3 to 23.

The following figures show the best and worst cases of lateral placements. In the first there was no lateral variation in the position of the vehicle while in the second there was completely random variation along the section. This lateral placement variation has a significant impact on the rut depths resulting from any profilometer survey.

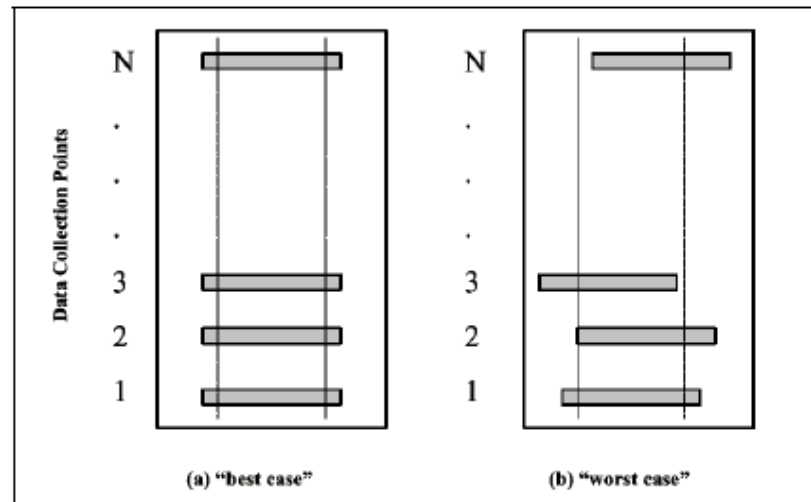


Figure 2.27 Impact of the Different Lateral Placement on Rut Depth

So only optical and laser scanners are accepted. Yet they have their own shortcomings in the real application. Both of them are very high in the costs. The optical products cost around \$70,000 and laser scanners such as the product from the Mandli cost around \$300,000, which is out of reach of many customers. This calls for an accurate yet affordable laser scanner that can be widely used in the future measurement of rut depth. The device that is proposed by the author of the thesis is AR4000 laser scanner.



## CHAPTER 3

### SYSTEM DEVELOPMENT

#### 3.1 System Requirements

##### 3.1.1 Commercially Available Scanners

There are many types of scanners available in the market which were mainly designed and sold for commercial purposes. The researcher conducted internet search on lots of available scanners, reviewed each product in detail and contacted each individual producing company for specifications for each type of scanner to try to find the one that would work best for the purpose of the research.

Table 3.1 lists the commercially available scanning laser rangefinders that were considered. The predominant ranging method is pulse time-of-flight. A laser beam pulse is emitted and reflected off an object. The scanner's receiver detects the reflected light energy, and the time between transmission and reception is measured and converted to distance.

Table 3.1 Comparison of Commercially Available Scanning Laser Rangefinders

Manufacturer		Acuity	Sick	Riegl	Riegl	Cyra
Model	-	AR4000-LIR	LMS-200-30106	LMS-Z210	LMS-Q140i-80	Cyrax 2400
Mass	kg	1.6	4.5	13	6	29.6
Volume	cm <sup>3</sup>	2,600	4,500	15,000	14,800	63,300
Power	W	23.5	17.5	54	30	125
HFOV	degrees	± 150	± 180	± 170	± 40	± 20
VFOV	degrees	-	-	± 40	-	± 20
Spacing	degrees	0.18	0.5	0.24	0.14	0.04
Divergence	mRad	0.5	5	3	3	0.06
Horizontal scan rate	Hz	45	40	10	10	2
Sample frequency	Hz	100 - 50,000	27,000	5,500	5,500	800
Range	m	0 to 15	2 to 15	0 to 8	0 to 8	0.5 to 50
Deviation (at max range)	mm	0.5	5	15	15	6
Laser safety class	-	IIIb	I	I	I	II
Ranging method		Time of flight	Time of flight	Time of flight	Time of flight	Time of flight
Mechanism		Rotating mirror	Polygonal Mirror	Rotating Sensor	Polygonal Mirror	Dual Mirror

After careful consideration from all aspects, the AR4000 excels from the groups of scanners and is selected by the researcher as the scanner for the project not only because the power AR4000 presented as compared with other scanners, but also because it is more affordable than other scanners for the research purposes.

The researcher wants to install the laser scanner at the rear of the vehicle with the distance from pavement to the equipment near 6feet, and the scanner area may cover the whole lane, more than 12 feet. The rut usually ranges only more 5mm, so the accuracy of the scanner needs to be less than 1mm. Also because the vehicle is moving in 40-60 mph, we need it can scan 100 points in each lane and more than 1000 points per second. As to the price, it is favorable that the whole equipment is less than \$10.000. AR4000 seemed to satisfy these requirements and therefore was chosen by the research. In the following section, AR4000 scanner was described in detail.

### **3.1.2 AR4000 Laser Scanner**

The AccuRange 4000 laser rangefinder is Acuity's longest distance measuring tool. Employing time-of-flight measuring principles, the rangefinder can accurately gage distances up to 54 feet (16.45 m).

Non-contact measurement is made simple with the three models within the AR4000 rangefinder series. All models are compact and durable, residing in a NEMA-4 enclosure for challenging industrial environments.

Acuity's rangfinders are very unique distance measuring devices. They employ a modified time-of-flight measurement principle that leads to very fast and accurate measuring speeds.

The AR4000 differs from other long-distance rangefinders in that the laser emitter and return signal collection lens are concentric. The illustration (figure 3.1) below reveals the major functionality of the rangefinder. A collimated beam of laser light is emitted from a diode in the center of the fresnel collection lens. Light hits a target and is diffusely reflected, collected by the lens and focused on an avalanche photodiode.

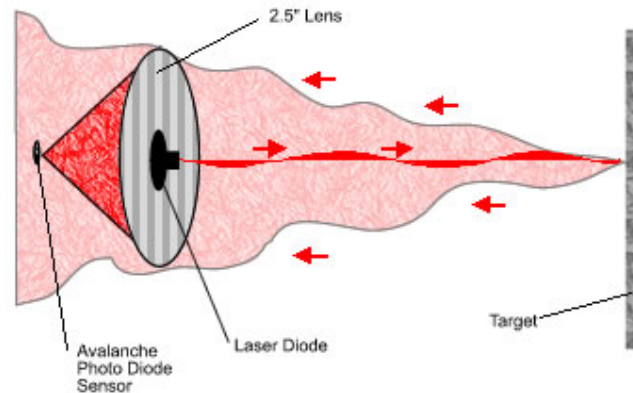


Figure 3.1 The Mechanism of the Rangerfinder

Because the emission and collection is concentric, the AR4000 rangefinder can be used to measure down narrow opening and tubes.

The AR4000-LIR laser rangefinder (figure 3.2) has a working range to 54 feet on light surfaces (85% diffuse reflectance, such as paper or light paint) or 35 feet on a 30% reflectance target with an accuracy of 0.1 inches. It uses an infrared 780 nm 8 milliwatt laser. This is the sensor of choice for best accuracy in most applications. An

optional 20 m W laser upgrade is also available for the AR4000-LIR sensor with an accuracy of 0.2 inches, for extended range to darker surfaces (54 feet on 30% reflectance) and in sunlight.

The AR4000-LV rangefinder has a working range of zero to 40 feet on 85% diffuse reflectance surfaces or 30 feet on a 30% reflectance target with an accuracy of 0.3 inches. It uses a visible 670 nm 5 milliwatt laser. This is the sensor of choice where a visible beam spot is required or your application must remain under and FDA Class IIIb laser category.



Figure 3.2 AR4000-LIR Rangefinder

The AccuRange Line Scanner (figure 3.3) is precise spinning mirror assembly that when coupled with Acuity's laser rangefinder, creates a laser scanner. The laser scanner sweeps a laser spot through a 360° rotation for the measuring of profiles and scenes. The AccuRange line scanner is often further integrated to create a 3D laser scanner.



Figure 3.3 AccuRange Line Scanner

The AccuRange™ Line Scanner can be used with the AccuRange 4000 to scan and collect distance data over a full circle. The scanner consists of a balanced, rotating mirror and motor with position encoder, and mounting hardware for use with the AccuRange 4000. The scanner deflects the AccuRange beam 90°, sweeping it through a full circle as it rotates. The standard encoder resolution is 4096 counts per revolution. The basic description of the AccuRange 4000 and AccuRange High Speed Interface is listed by the following bullets.

- Scan rates up to 2600 lines per minute.
- Scanning mirror sweeps laser beam through 360° and returns reflected light to AccuRange 4000.
- 96% optical reflectance for maximum sensitivity
- Compact, lightweight assembly with AccuRange 4000.
- May be used with AccuRange 4000 or AccuRange 4000 and AccuRange High Speed Interface
- Motor encoder with 2000 position counts/revolution and index pulse.



Figure 3.4 Laser Scanner with the Mirror

The Acuity laser line scanner has an elliptical mirror situated at a  $45^\circ$  angle to deflect the outgoing laser spot and the return signal (figure 3.5). The mirror is engineered the highest optical standards with 96% reflectance.

Using the High Speed Interface Card , the line scanner can sample up to 200 KHz. With a maximum mirror rotational speed of 2600 rpm, the line scanner can sample 4615 distance measurements per revolution.

Typically, engineers will use the AR4000-LIR rangefinder in conjunction with the line scanner because the LIR can measure to most surfaces in most conditions. Although the AR4000-LIR is a Class IIIB laser product, the laser class CAN BE reduced when operated with the line scanner. The line scanner sweeps the laser spot at very high speeds and the effective power is reduced. So long as the mirror is always spinning, the radiation danger to the human eye is reduced to the levels of a Class I laser (eye-safe). In these cases, the integrator is responsible for safety interlocks to guarantee that the laser is disabled until the mirror spins.

### 3.2 System Improvements

After the test use of the AR4000 scanner, some problems of the existing scanner came up. One of them is that when using the AR4000 in the sun, the data collected are distorted. Another case of data distortion is when the road is dark. We reflected the problems that we have encountered in the process of AR 4000 application to the company and suggested the improvements of the system. They agreed to do so and months later, they provided us with an improved AR4000 laser scanner.

The new line scanner enclosure is a NEMA-4 housing for the AR4000 with Line Scanner and the AR4000 power supply. It has a field of view of 90 degrees. The window is anti-reflection coated window mounted at an angle that prevents reflections from returning to the mirror or to the sensor face (figure 3.5).

For use in ambient temperatures above 80 F, it is available with a cooling fan or can be used with externally supplied cooling air. The enclosure is available in gray painted steel or brushed stainless as show in figure 3.6 and 3.7.

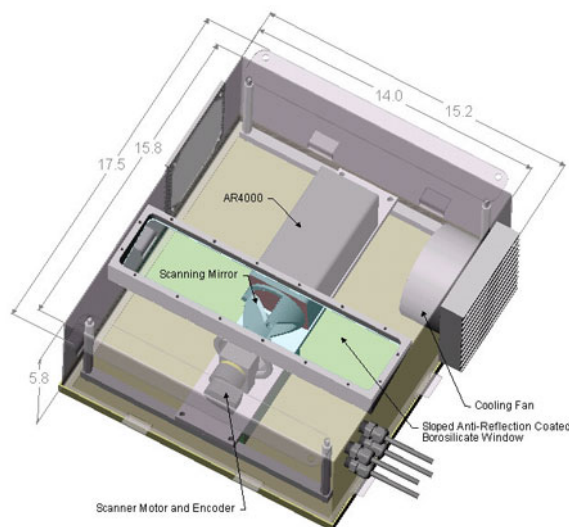


Figure 3.5 The Developed Scanner



Figure 3.6 The Exterior Appearance of Improved Scanner

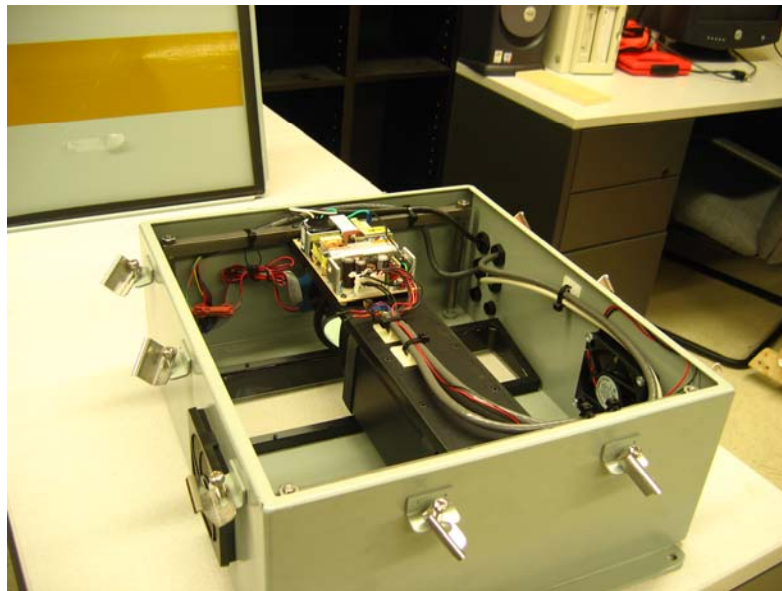


Figure 3.7 The Interior Appearance of Improved Scanner

The high power 20 mW laser diode option is only available for the AR4000-LIR model. It is recommended for measuring to dark targets at ranges beyond 30 feet, or in outdoor applications where the target surface may be sunlit. The high power laser has twice the drift and fluctuation in the range readings of the 8 mW version, so it is



half as accurate as the 8 mW version, but it often works in situations where the lower power laser is not sensitive enough. The laser class remains IIIB.

The High Power Laser Option is typically designated during manufacture. Changing the laser on an existing sensor entails additional cost, as it requires significant changes and recalibration. The lifetime of the laser diode is 50,000 hours.

### 3.3 System Testing

The rationale behind the hardware development is that the scanner covers 135 degrees of the pavement profile and laser scanner position above the road. The working mechanism of the laser scanner was shown in the figure 3.8.

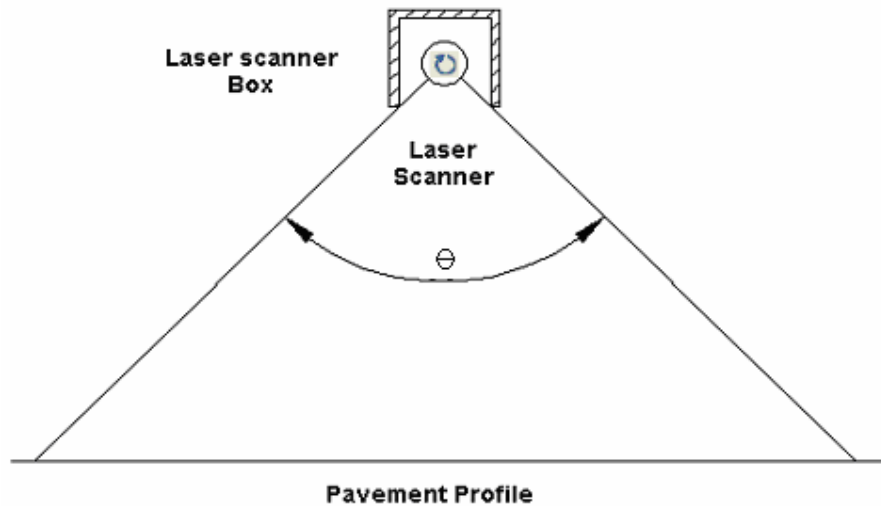


Figure 3.8 The Working Mechanism of the Laser Scanner

Based on this rationale, a wooden frame was made by the researcher of the project to test the functionality of the laser scanner. As you will see in the following picture (figure 3.9 and 3.10), the four-legged frame holds the scanner on the top flat plane of the frame. The scanner on the top was connected with computer and monitor

for data collection and transmission. Once the scanner is turned on, the profile data in the form of Excel spreadsheet will automatically transmit to the computer for later data analysis.



Figure 3.9 Installation of the Frame and the Scanner



Figure 3.10 On Site Measurement

### 3. 4 Software Development

Software plays a very important role in the data analysis process of the project.

The software used in this project is developed in Visual Basic and performs the data analysis on PCs with a series of windows operating systems.

The main function for the software is for data analysis. By using the analysis functions of the software, the researcher can easily plot the data sets, make the analysis of it and get the results of the analysis. The following figures are the interface of the software. Figure 3.11 shows the interface of the software for data collection, figure 3.12 and 3.13 are the examples of data sheets.

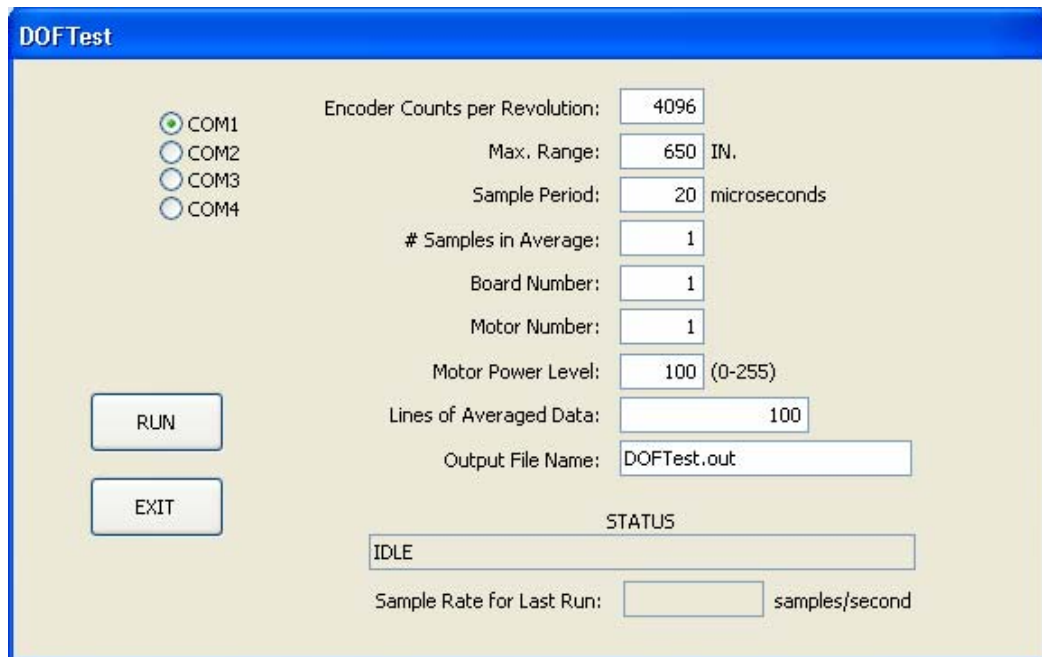


Figure 3.11 Interface of Data Collection Software

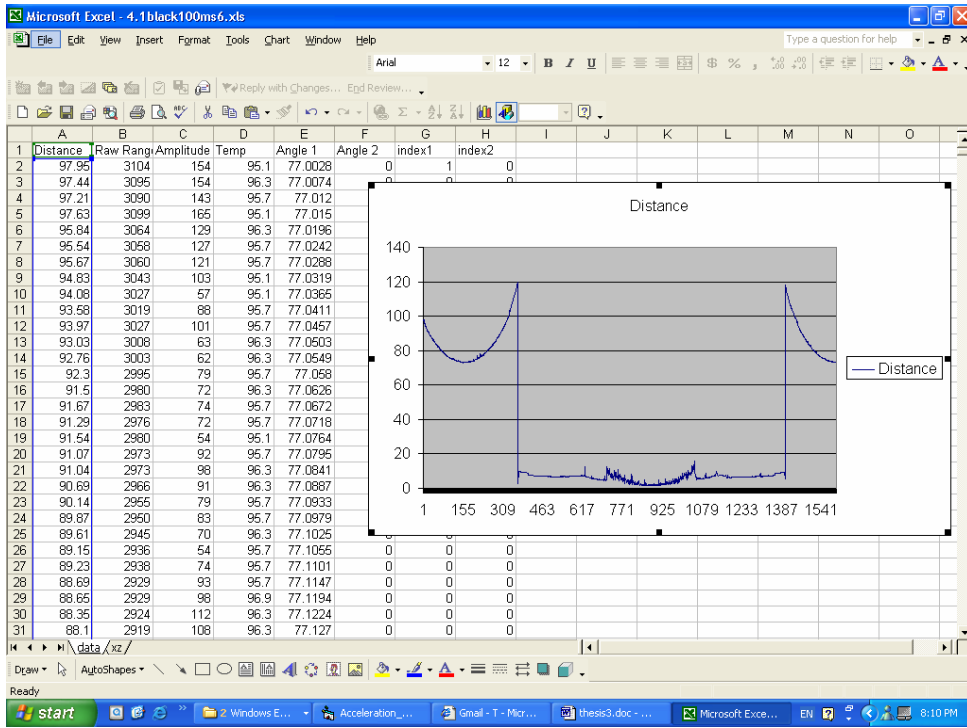


Figure 3.12 Interface of Data Sheet (1)

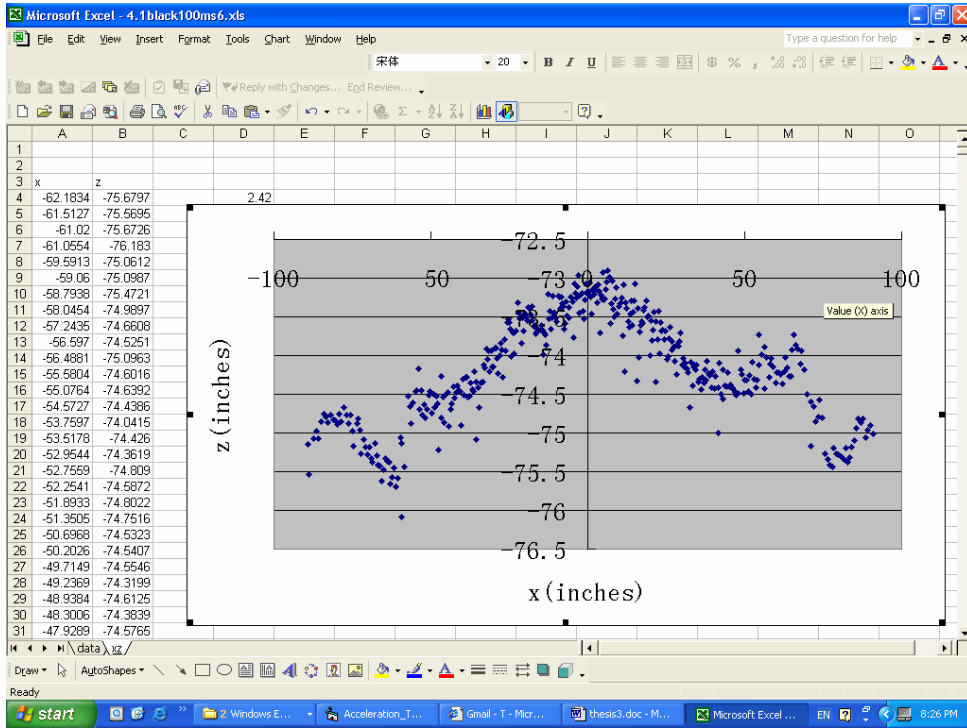


Figure 3.13 Interface of Data Sheet (2)

## CHAPTER 4

### METHODOLOGY

#### 4.1 Calibration

Calibration is required due to the errors generated by the system and the characteristics of the floor quality. Factory calibration was done in the way as shown in the following figures (figure 4.1 and figure 4.2). Due to some technical difficulty, factory calibration cannot be performed by the user of the scanner. And also factory calibration may not be accurate for the measurement of rut depth in the real road situation. Therefore, the researcher calibrated the scanner in two ways to see the functionality of the scanner in real situation.



Figure 4.1 Demonstration of Factory Calibration

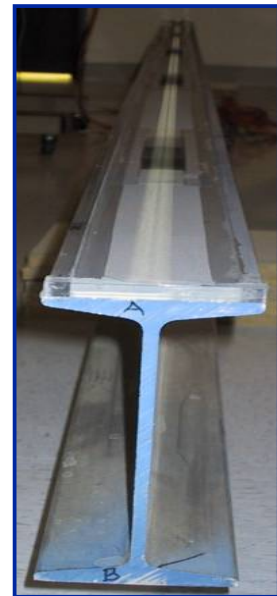


Figure 4.2 Standard Plane

First of all, the researcher tested the calibration on a flat floor surface. After scanning the flat floor surface, a reference profile was obtained. The analysis of this reference profile showed that the calibration is somewhat accurate by using the scanner. In the following figure (figure 4.3), you can see that the scanning result turns into somewhat a straight line because of the scanning surface being a flat floor.

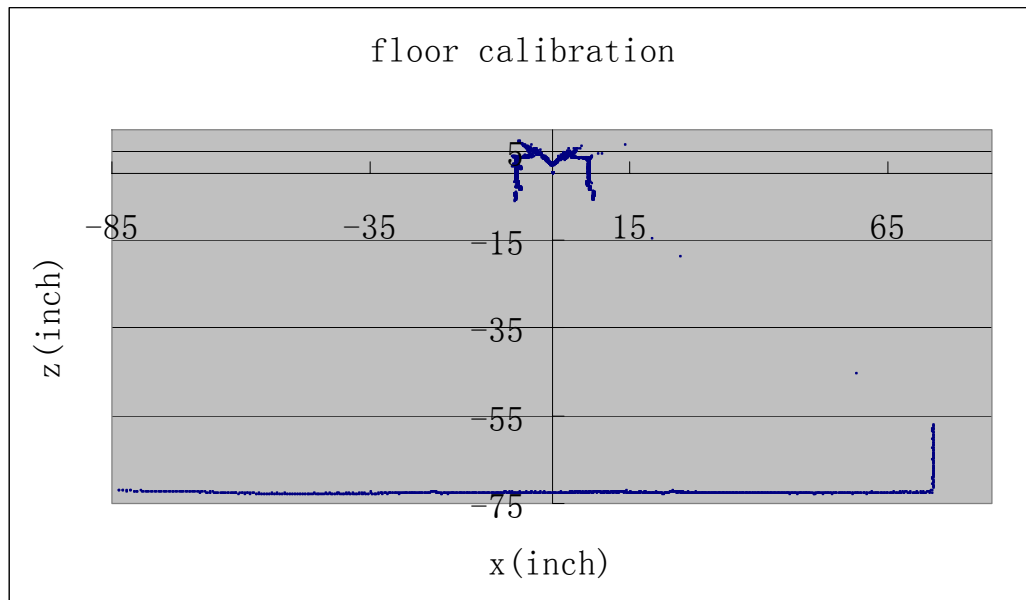


Figure 4.3 Results of Floor Calibration

Yet the calibration is not ideal by using the scanner which will be obvious when the testing results were shown in a more closed look (figure 4.4). As shown in the figure 4.4, you can see that when looking closely from the point of only one inch distance difference, the result is not a straight line, which are also indicated in the linear regression tables below (table 4.1 and table 4.2). Instead, it waves around the straight line. After careful consideration and discussion with the professor and contact with people from the factory, we decide to ignore this shortcoming because the reason for such an imperfect result may be due to the fact that the shiny epoxy surface of

the floor itself has too much glare which might to some degree influence the performance of the scanner. Anyway, we can get a somewhat straight line when using the scanner to scan the flat floor surface.

Table 4.1 Summary Output of Linear Regression

SUMMARY OUTPUT	
Regression Statistics	
Multiple R	0.021490342
R Square	0.000461835
Adjusted R Square	-0.002276626
Standard Error	0.162360127
Observations	367

Table 4.2 ANOVA of Liner Regression

ANOVA					
	df	SS	MS	F	Significance F
Regression	1	0.004445687	0.004445687	0.16864759	0.681557514
Residual	365	9.621696006	0.026360811		
Total	366	9.626141693			

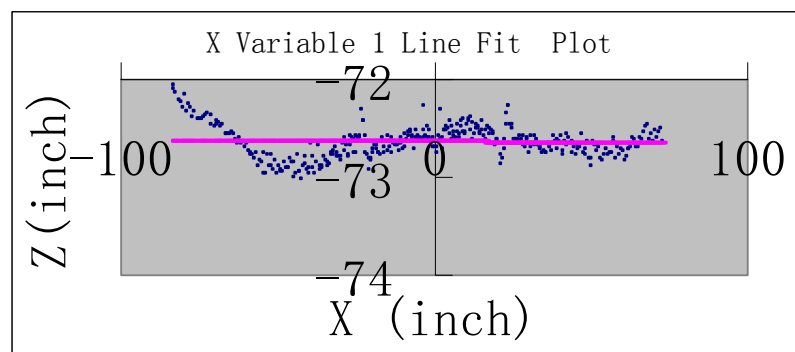


Figure 4.4 The Curve of Linear Regression

In addition to scanning the flat floor surface, predetermined shapes are placed on the floor to simulate significant profile shape. In this case two layers wooden



boards were placed together. Two smaller boards with the same size were placed on the top of the one big and long board. The height for lower layer board was 0.85 inches and the heights for the two smaller boards were 0.5 inches. Another reference profile was obtained in this situation and the result is indicated in the figure 4.5. We can roughly see from the following figure the height difference of each board. The result obtained from this scanning performance is not a line, which makes the analysis harder. The researcher then decided to measure the moving average of the boards. The result (Figure 4.6) showed a line shape and indicated clearly the moving average.

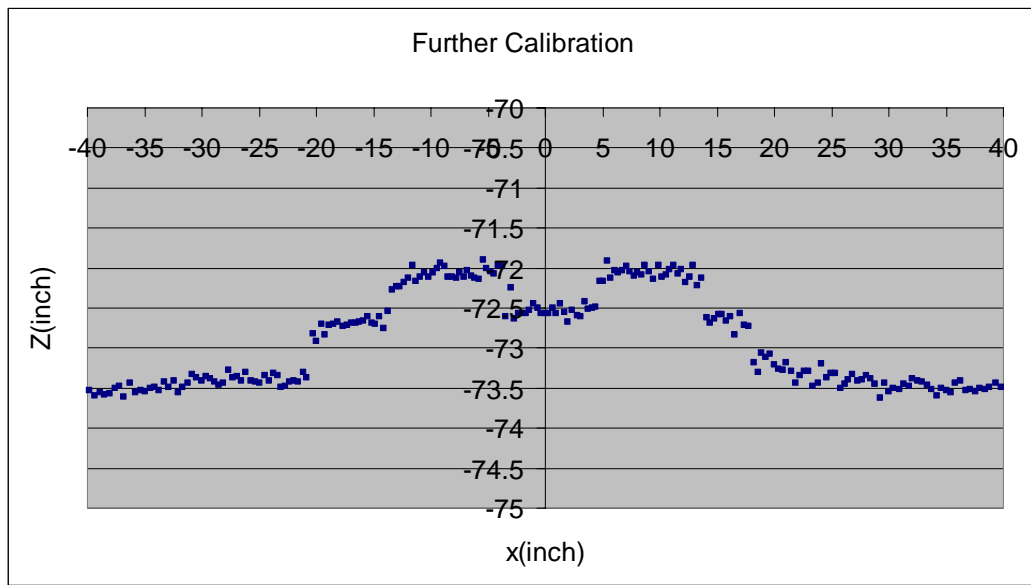


Figure 4.5 The Scanning Results with 2 Layered Boards

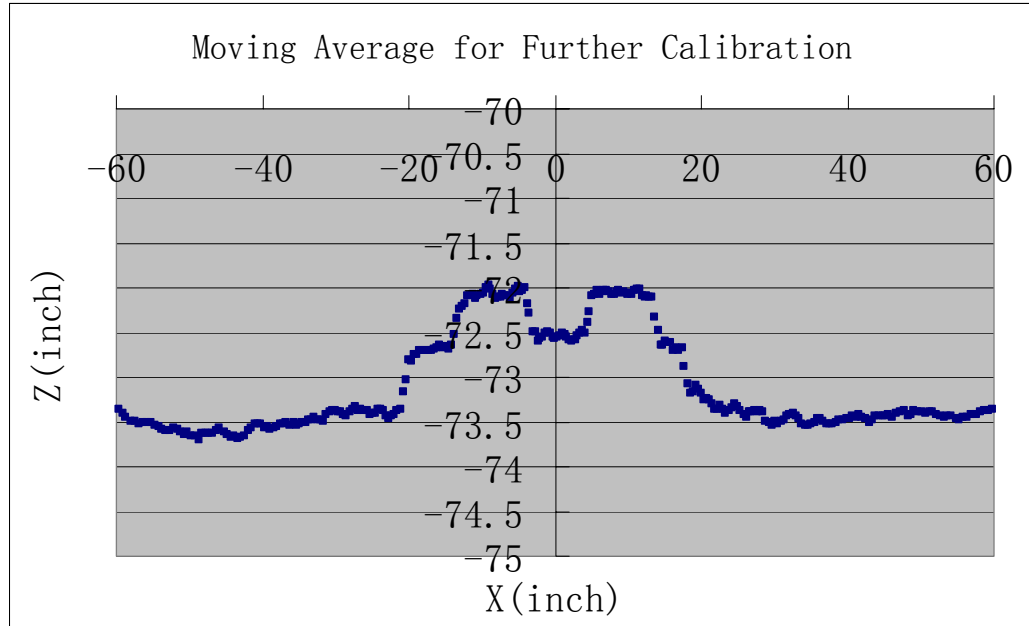


Figure 4.6 The Moving Averages of the Two Layered Boards

From the above two figures, the average height of the bottom layer board was 0.79 inches and the average heights of the top layer boards were 0.54 inches, which were to some degree different from the real heights of the boards. The difference between them with the real boards were  $-0.06$  and  $+0.04$  respectively. The average error was 0.05 inches, which was around 1mm. So it can be said that the measuring result should be considered accurate.

From the above analysis, it is obvious that although AR4000 laser scanner is not 100 percent calibrated in the real measurement of rut depth, it is applicable in the project and will provide accurate and useful result for the study.

#### 4.2 Analytical Process

There are three basic algorithms used for calculating rut depths. They are the straight-edge, wire and pseudo-rut models.

### 4.2.1 Straight-Edge Algorithm

The *straight-edge* model emulates the manual method of placing a straight-edge across the pavement. Figure 4.7 is an example of the straight-edge model.

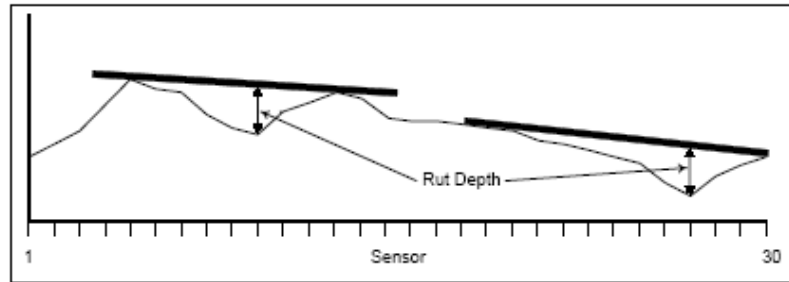


Figure 4.7 Example of Straight-Edge Simulation

The straight-edge rut depth algorithm was based on the SHRP algorithm in Hadley and Myers (1991). The analysis starts at sensor 1 which is the reading closest to the pavement kerb. It progresses until the rutting in one wheelpath is established. It is then repeated for the second wheelpath starting at right-most sensor and moving downwards.

To illustrate the analysis process consider Figure 4.8-A which shows a set of hypothetical transverse profile elevations. The algorithm places the end of the straight-edge at a starting point. For each start point, the slopes are calculated between it and all successive points which would fall within the span of the straightedge.

Figure 4.8-B illustrates this using Sensor 3 as the start point. The maximum of these slopes is identified (Sensor 5 in Figure 4.8-B).

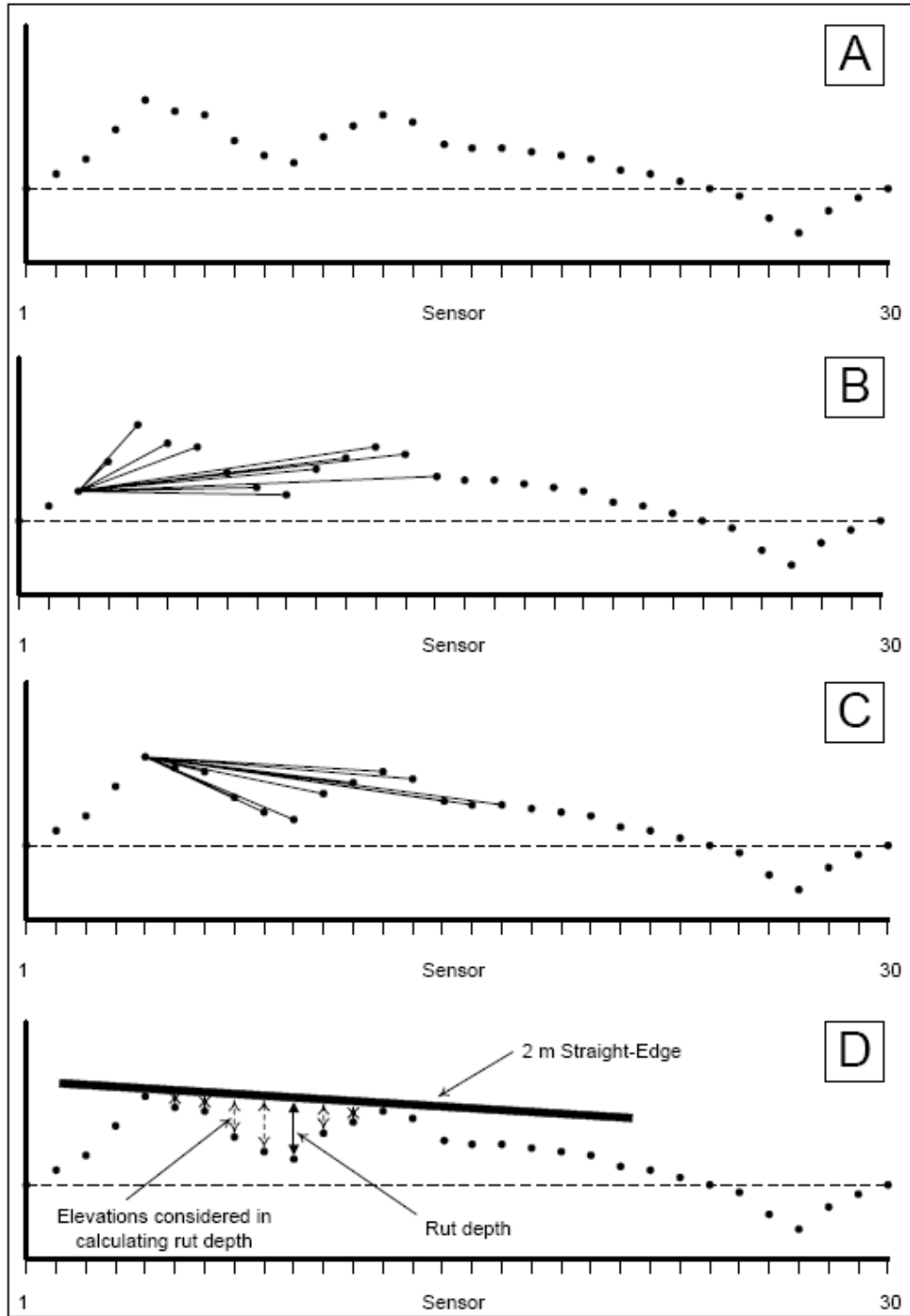


Figure 4.8 Example of Calculating Rut Depth

Two criteria are used to establish whether or not this is a viable placement point for calculating a rut depth. If either of these are met the current starting point will not

produce a rut depth and the analysis moves on to the next starting point. These criteria are:

- if the maximum slope is less than the slope between the start point and the preceding sensor; or,
- if the maximum point arises for the point adjacent to the starting point.

Once a viable placement point has been established, the vertical distance of all intermediate placement points is established. In Figure 4.1-C the start point is Sensor 5 and the maximum slope point is Sensor 13. Here, the maximum slope is that closest to the horizontal plane since all elevations are below that of Sensor 5. Figure 4.1-D shows the various possible rut depths for these two points.

For that starting point, the rut depth is the maximum of the vertical distances of all intermediate points. It should be noted that in calculating the rut depth the change in horizontal span due to tilting is assumed not to be significant.

For each possible starting point a maximum rut depth is derived. The largest of these values is taken as the rut depth for the wheelpath in question.

#### **4.2.2 Wire Model Algorithm**

The wire model algorithm connected the high points on the profile and established the rut depth under these points. As described by Cenek, et al. (1994), the *wire model* is popular since it is fast in performing calculations. Figure 4.9 is an example of such a calculation. Unlike the straight-edge, the wire model expresses the rut depth based on a wire stretched over the high points. The distance to the pavement from the wire is calculated and the highest values constitute the rut depth.

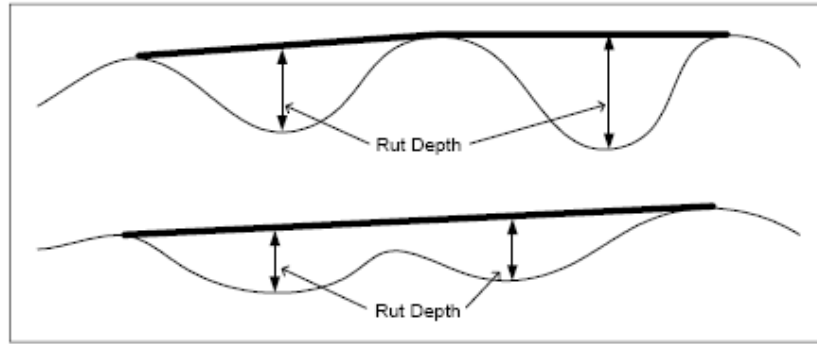


Figure 4.9 Example of Wire Model

### 4.2.3 Pseudo-Rut Algorithm

*Pseudo-ruts* are defined as the difference (in mm) between the high point and the low points. It is used on systems with only a limited number of sensors and, it is commonly used in the USA (figure 4.10)

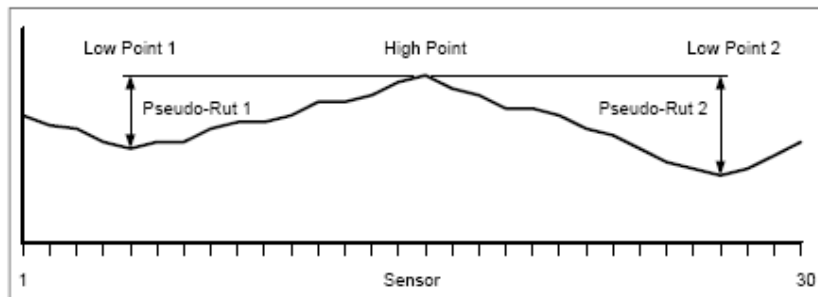


Figure 4.10 Definition of Pseudo-Ruts

Pseudo-ruts are calculated as the difference in elevation between the high and low points in the profile. In developing the pseudo-rut algorithm it was found that the results were very sensitive to the slope of the reference profile and that unless the data were 'normalized' so that the reference profile slope was eliminated, the statistic was not appropriate.

To illustrate this, consider Figure 4.11 which compares the pseudo-rut estimates with and without slope correction. The rut depth estimates are [25/16] vs. [43/7] for the two cases. Given the basis for the pseudo-rut statistic, the analysis was done using normalized profiles. These were created by adjusting the elevation readings, hereinafter referred to as ‘normalization’ so that the end elevation had the same value as the initial elevation—usually 0.

It should be noted that the nature of the straight-edge and wire model rut depth calculations do not necessitate normalization.

The HRD software can display either the normalized (default) or standard profile.

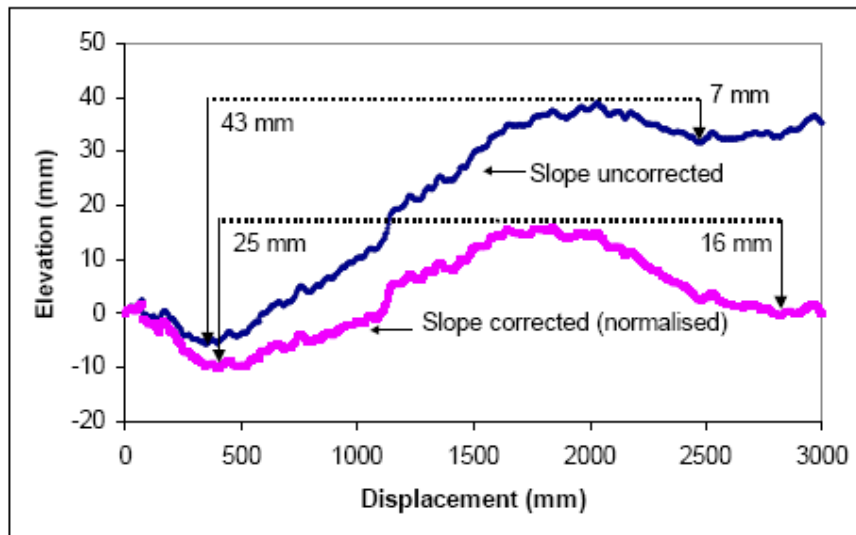


Figure 4.11 Implications of Slope Normalization on Pseudo-Ruts

### 4.3 Straight-Edge Model and Algorithms of the Study

Although the application of pseudo-ruts model is considered the easiest method in the computer-assisted environment, it is not selected by the researcher as the calculating methods in the study. Yet it is comparatively harder to get the exact value

of calibration. Therefore, the first model – straight-edge model and its corresponding algorithms are selected as the calculation method for this project. The main reason for this that not only is it pretty easy to apply in the computer-assisted environment and get accurate result, but also the calibration is easier to be conducted and the accuracy of calibration is relatively high. The following pictures (figure 4.12) shows the manual yet very efficient and accurate ways of calibration.

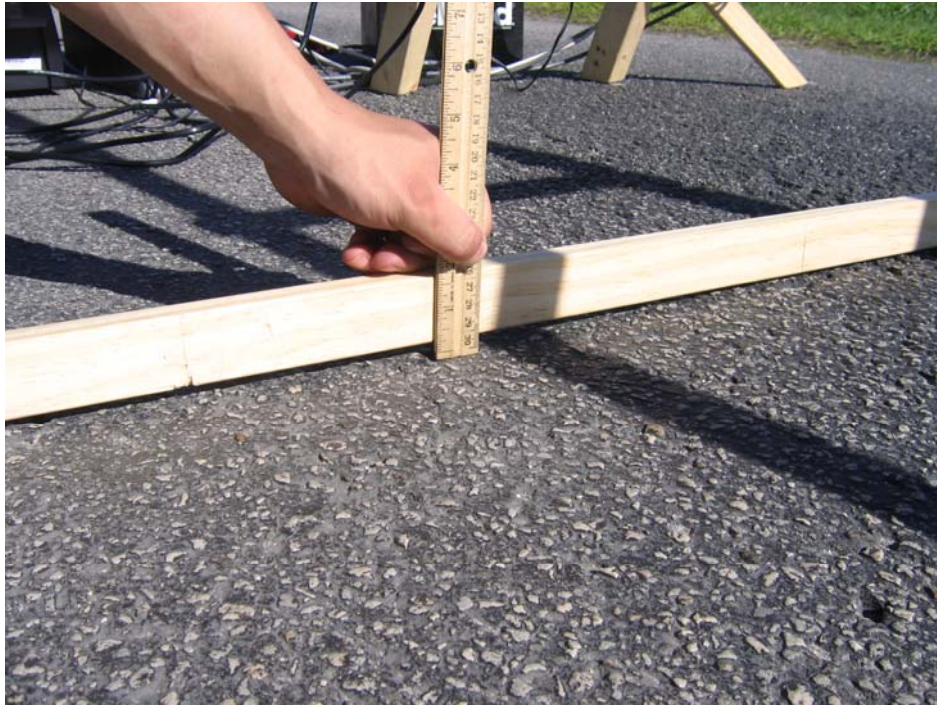


Figure 4.12 Picture of Using Straight-Edge Method for Rut Depth

Generally speaking, under straight-edge model, there are two options for measuring the rut depths. As shown in figure 4.13, they are: perpendicular to the datum of the elevation measurements or perpendicular to the straight-edge (or wire).



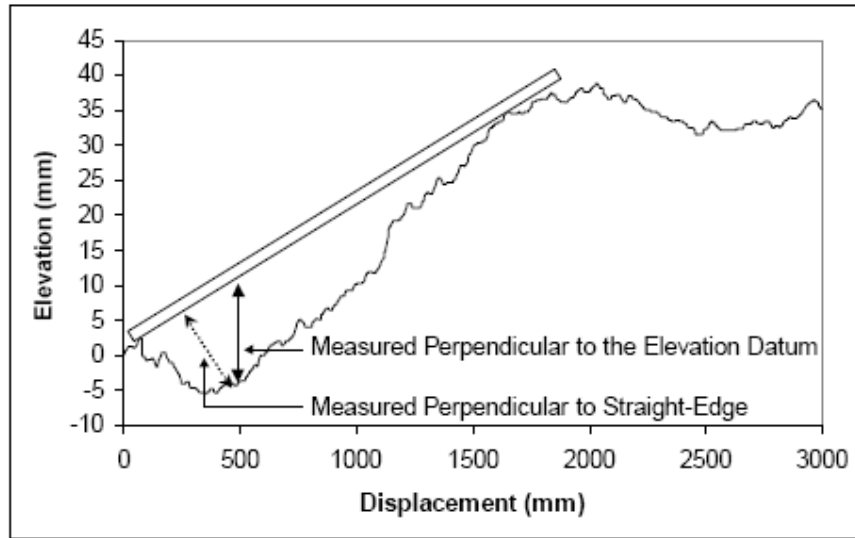


Figure 4.13 Implications of Straight-Edge Datum

The SHRP straight-edge algorithm takes the measurements as perpendicular to the datum so that is what was used in all analyses presented here. Another reason for using perpendicular to the elevation datum instead of perpendicular to straight-edge is because the former is easy to be measured and calculated.

To conclude, the straight-edge model is applied in the project and its corresponding algorithms are used for calculation of rut depth. This model gives the researcher the convenience to obtain the result of measurement relatively easily under computer-assisted environment, and its calibration process is old yet pretty efficient and works perfectly for the purpose of the study. Among the two options offered by straight-edge model, measurements as perpendicular to the datum are chosen over perpendicular to the straight-edge because of the convenience of the measurement and calculation.

## CHAPTER 5

### DATA COLLECTION AND DATA ANALYSIS

In this chapter, the process of data collection was introduced. The difficulty in this process and the considerations were mentioned to justify the data collection. The collected data then were analyzed by the software developed by the researcher of the project. Some conclusions based on the data analysis were derived accordingly.

#### 5.1 Data Collection

Data collection is one of the most important parts in the whole project, which can decide the success or failure of the project and serve as the basis from which the analysis is conducted and conclusions are drawn.

In order to get efficient data sets, it is better to do the field data collection in the busy road where high volume of traffic may make the measurement of rut depth more meaningful. Therefore, the researcher went to the Linebaugh Avenue for a whole day trying to collect the data of rut depth. Yet the result is unsatisfying because the busy traffic left the researcher no chance to collect data safely. The researcher has to give up the plan of collecting data from busy roads with obvious rut depth.

The researcher then spent a few days sightseeing the city of Tampa, trying to find a relatively quiet road where rut depth is measurable. After a few days' efforts, one small road located near an apartment complex close to USF is targeted and decided by the researcher to be the site where the data would be collected.

Data collection was finally conducted one day. All the equipments such as the frame, the laser scanner, the computer were transported to the site. Several locations on the small road were targeted and the frame was set up on the locations one after another. Once the location was targeted and the frame was set up, the laser scanner was turned on to collect the data particular to this location. The profiles were generated automatically once when laser scanner was operating. The profiles were saved in the Excel format in the computer. The same procedure was repeated for several times to get the data for multiple locations. The following figure showed an example of generated profile in the format of Excel spreadsheet.

## **5.2 Data Analysis**

Data analysis was conducted in actually six steps.

### **5.2.1 Data Sheet**

After field data collection, data sheet were generated in the format of Excel spreadsheet. Several columns of Excel spreadsheet are useful in our data analysis. For the purpose of this particular research, we paid special attention to the column of Distance and column of Angle 1 (as shown in figure 5.1). By using these two columns, an absolute coordination system was set up taking the laser as the original point.

The changing regularity of distance is easily obtainable from the data sheet. When the laser is scanning in the box, the distance is smaller, and when the laser is scanning in the working area, the distance changed bigger suddenly. Because the height of the scanner is fixed, the distance altered as the scanning angle changed.

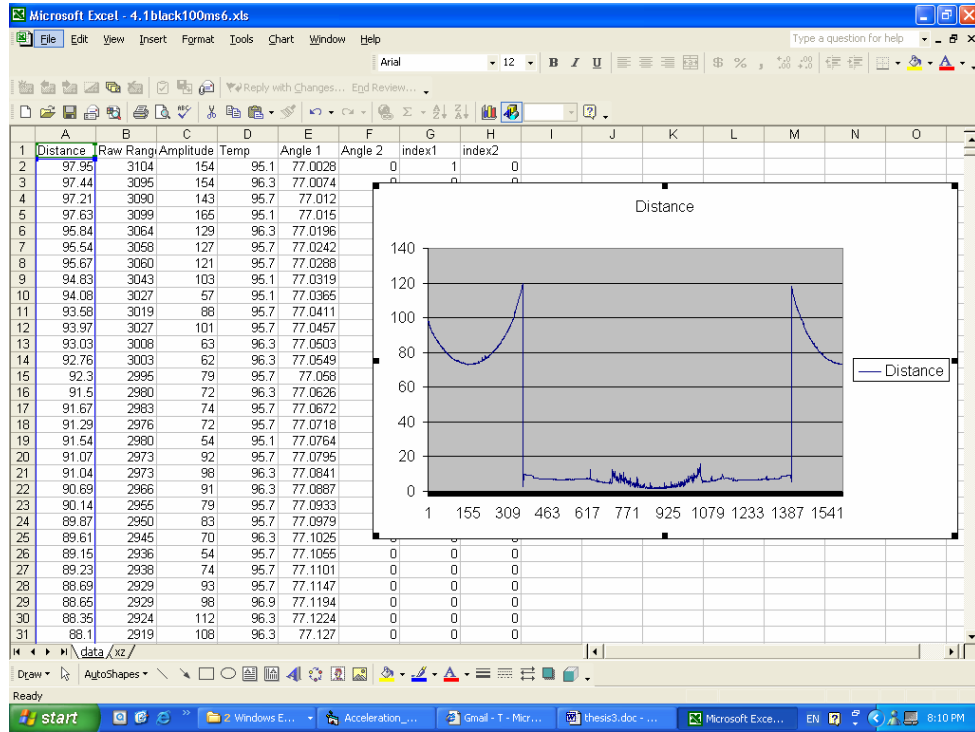


Figure 5.1 Sample Data Sheet

From these two parameters: distance and angle 1, we can decide of the position of each point in the coordinator. The method of calculation is as follows:

$$X = \text{Distance} * \cos(\text{Angle1} + \theta)$$

$$Z = \text{Distance} * \sin(\text{Angle1} + \theta)$$

By using this calculation method, the position of every point of data was decided on the coordinator. And the polar coordination system was changed successfully to the 90 degree angle coordination system.

### 5.2.2 Initial Angles

During the scanning process, the distance between the scanner and scanning points is different. The shortest distance is when the scanner scans in the box, whereas the longest distance is when the scanner scans the floor. During the scanning process,

we can get the first point when the scanner started scanning the floor and the last point when the scanner finished the last scanning point on the floor. These two points are represented by two angles:  $\theta_1$  and  $\theta_2$  (figure 5.2). The initial angle is easily calculated by applying the following formula:

$$\theta = (\theta_2 - \theta_1) / 2$$

Following the same logic, all the angles of floor scanning can be calculated.

$$\sum \theta_n = (\theta_{n+1} - \theta_n) / 2$$

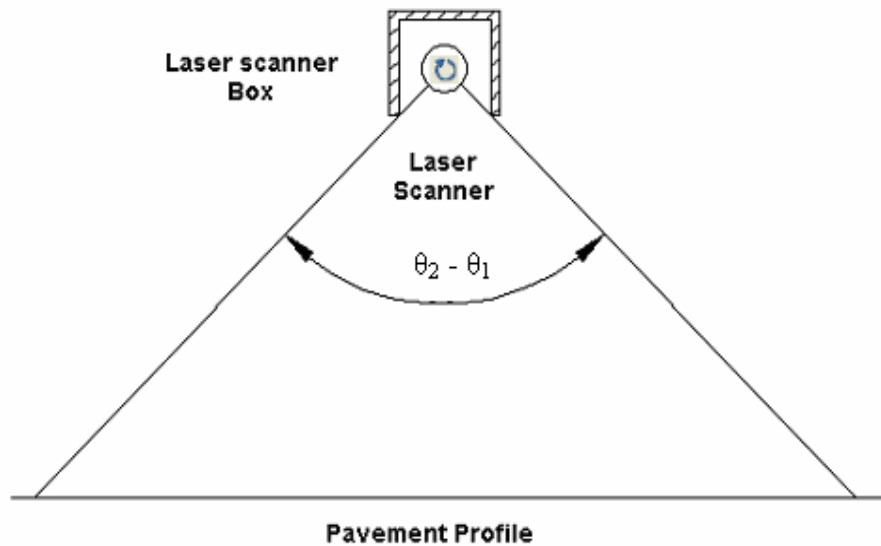


Figure 5.2 The Mechanism of Initial Angles

### 5.2.3 Scope Line

The initial analysis of collected data showed that when the road surface is dark, the data were discrete points as shown in the following figure (Figure 5.3). From the figure, it was clear that most of the points were gathered around 70 inches. Yet some of points reached the value of around 300 inches, which was obviously distorted. The

reason for this difference may be the ability to reflect the light was different for light pavement asphalt and dark pavement asphalt.

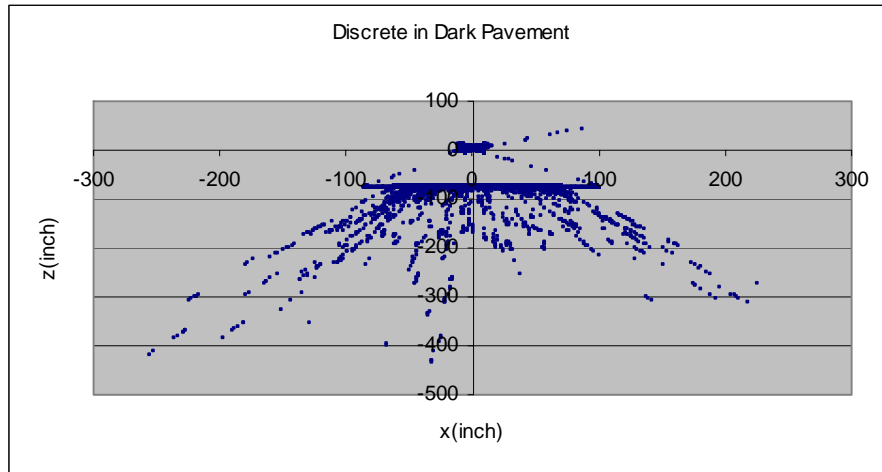


Figure 5.3 The Data Discretion in the Dark Pavement

But we can still see the basic shape of the profile as indicated in the figure 5.4.

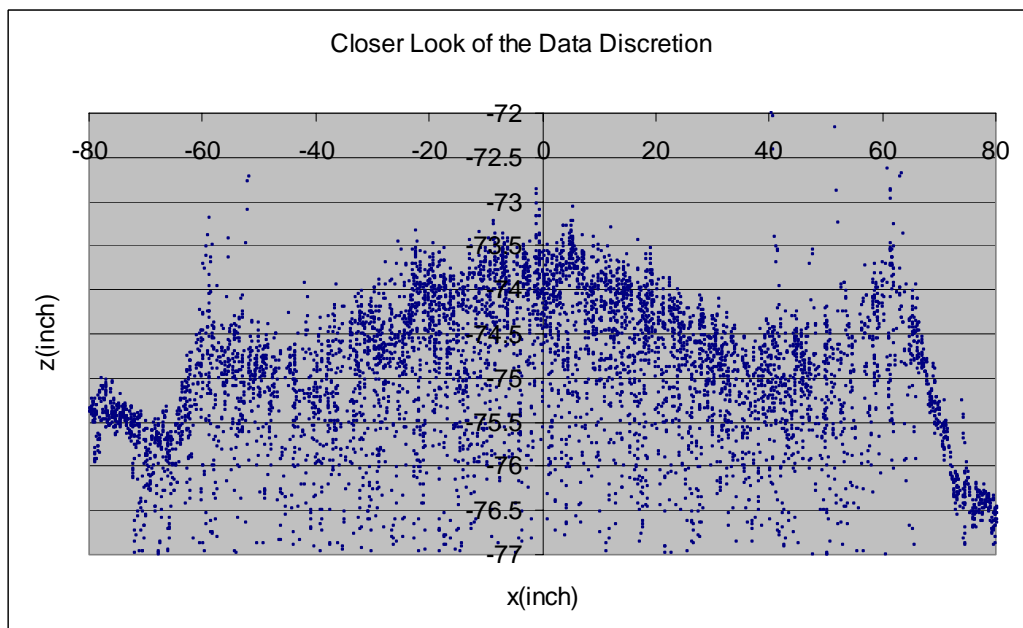


Figure 5.4 A Closer Look of the Data Discretion

So we developed one method to get the scope line of the profile of the pavement.

The purpose of this method is to filter the data. The scope line is developed based on

the coordinator with x value and z values as described in data sheet of profile.

Suppose there are  $m \times n$  data points in one segment of profile. The basic method is to put  $m$  number of points in a group; therefore, there are  $n$  groups with  $m$  points in each group. In each group, the maximal  $z$  value is chosen as the representative of the group. All the other points are ignored for the purpose of this study. That is to say, the number of maximal value is  $n$ . In this way,  $m \times n$  number of points are effectively reduced to  $n$  number of points. When all these  $n$  number of points are connected, it is obvious that the line kept its original shape (figure 5.5). This shows that this way of filtering did not distort the data in any major way and at the same time eliminated the discrete points to have a more favorable result.

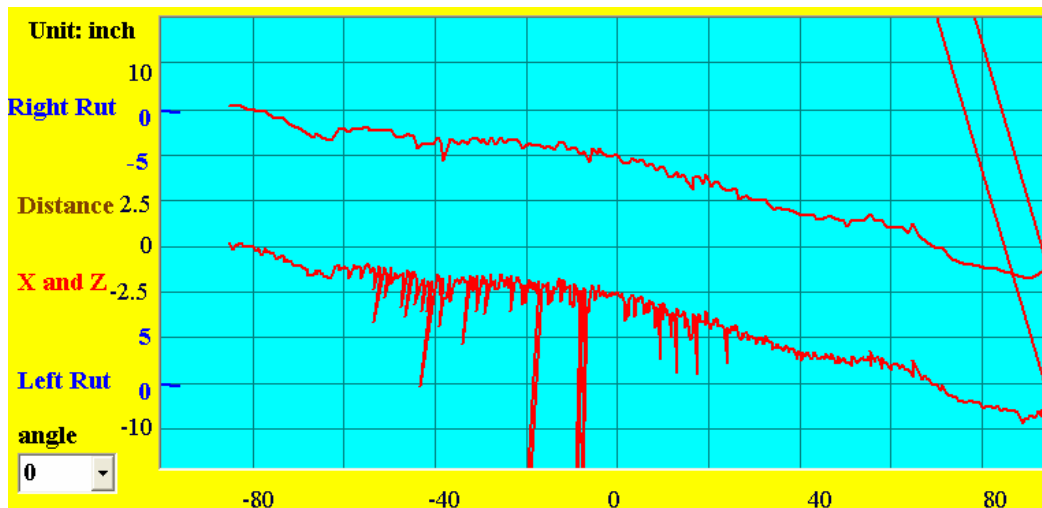


Figure 5.5 The Comparison between the Original Ling and the Scope Line

#### 5.2.4 Moving Average

In order to further improve the accuracy and make the curve smoother, the method of getting moving average is taken. The average of every three adjacent points is calculated and the average will serve as the value which was represented in the

coordinator. The calculation formula of moving average is as follows:

$$Z_n = \frac{\sum_{n-i}^{n+i} Z_n}{2i+1}$$

When the value of  $i$  equals 1, the formula changed to:

$$Z_n = (Z_{n-1} + Z_n + Z_{n+1})/3$$

The value of  $i$  can be changed from 1 to  $i$ . In this way, we can get more accurate data set. The number of points would change only slightly. The total number of points still was  $n-2$  because it was impossible to get the moving average for the very first and very last points in the scanning working area. By using moving average, almost every point was re-represented by an average. Points in the data set were more accurately represented the real situation and the smoother curve was obtained.

### 5.2.5 Analytical Process

All the other disturbing factors were eliminated or treated at this stage. It is time now to measure the rut depth. As we have discussed before in the methodology section, the calculation method of rut depth of choice is called straight-edge model. The values of slopes were calculated by using this model. More specifically, the values of slopes are measured perpendicular to the floor. After such a calculation, two maximal values and two minimal values were generated and the difference between the corresponding maximal value and minimal values of a slope was regarded as the two rut depths by two wheelpaths. The result of rut depth measurement is shown in the following figure (figure 5.6). Due to the fact that the installation of the



frame contains certain unavoidable angle errors, the curve we obtained was not totally flat. The researcher used certain method to flatten the line.

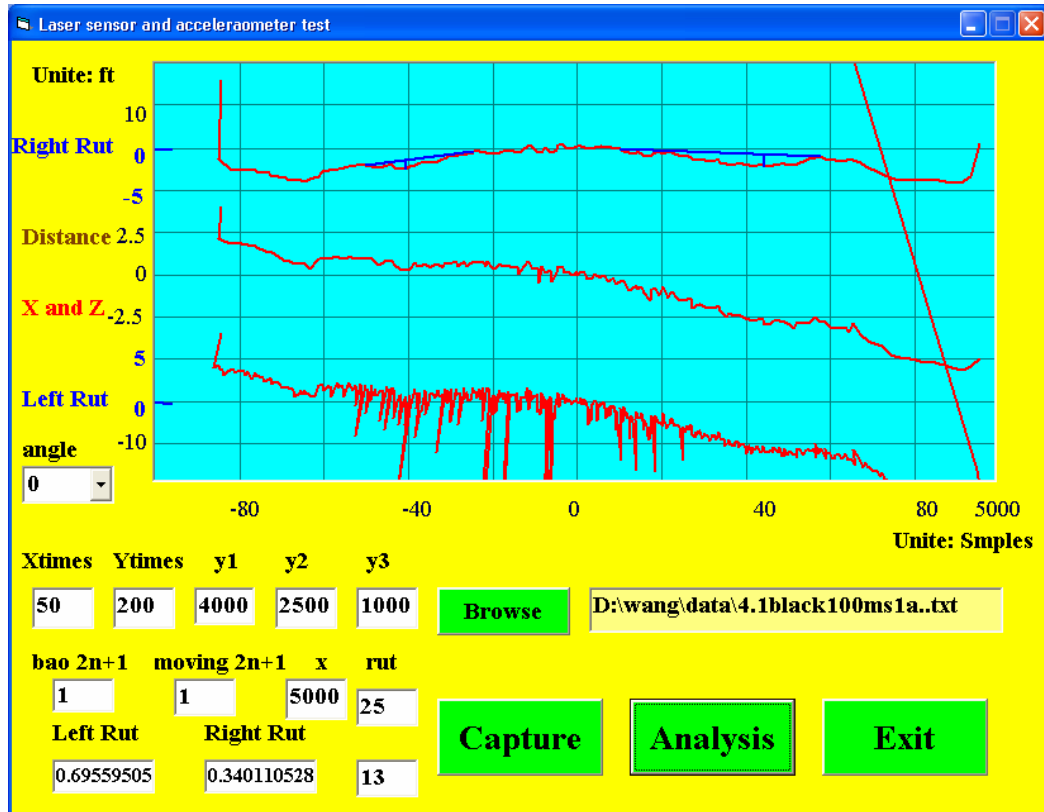


Figure 5.6 The Results of Rut Depth Measurement

## 5.2.6 Repeatability and Correlation

### 5.2.6.1 Repeatability

Repeatability means to obtain statistically similar results by using the same measuring device in the same measuring conditions. Repeatability represents one of the most important quality measures used for the evaluation of performance of a measuring device, in this case, the AR4000 laser scanner.

In order to test the quality of repeatability of the laser scanner, the measurement was conducted 10 times on the same spot. The result of each attempt was reported in

the following figure (figure 5.7). The similarity in the shape and values of each curve presented good repeatability.

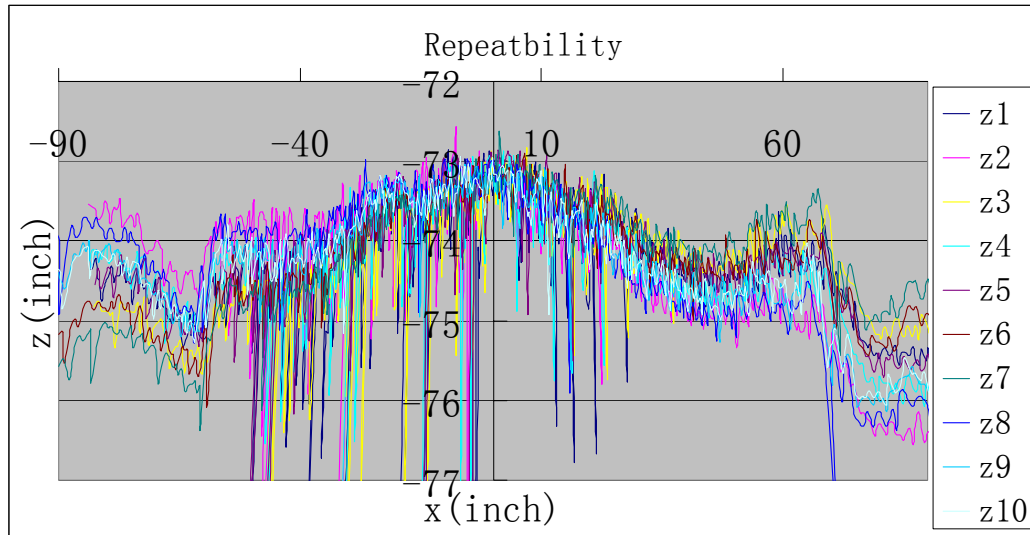


Figure 5.7 The Results of Repeatability Tests

### 5.2.6.2 Correlation

Correlation is another very important measure of the measuring device. Correlation is to some extent related with the measure of repeatability. If the quality of repeatability is high, it is usually true that the correlation is high. From the result of the repeatability of 10 measurements as shown in figure 5.10 to 5.19, it is clear that the accuracy is very high because when 10 measures generated the similar results.

In order to further test the correlation, the traditional manual method was taken as well (figure 5.8 and 5.9). The real measure of rut depth by using the ruler was compared with the result obtained by using the laser scanner. The comparison showed that the results were highly correlated by applying these two different kinds of measures. That is to say, the laser scanner can provide relatively accurate measuring results. Laser scanner should be favored by the researchers of rut related project

because its ability to obtain large amount of data in a short period of time with high accuracy.



Figure 5.8 The Manual Measurement of the Left Rut Depth

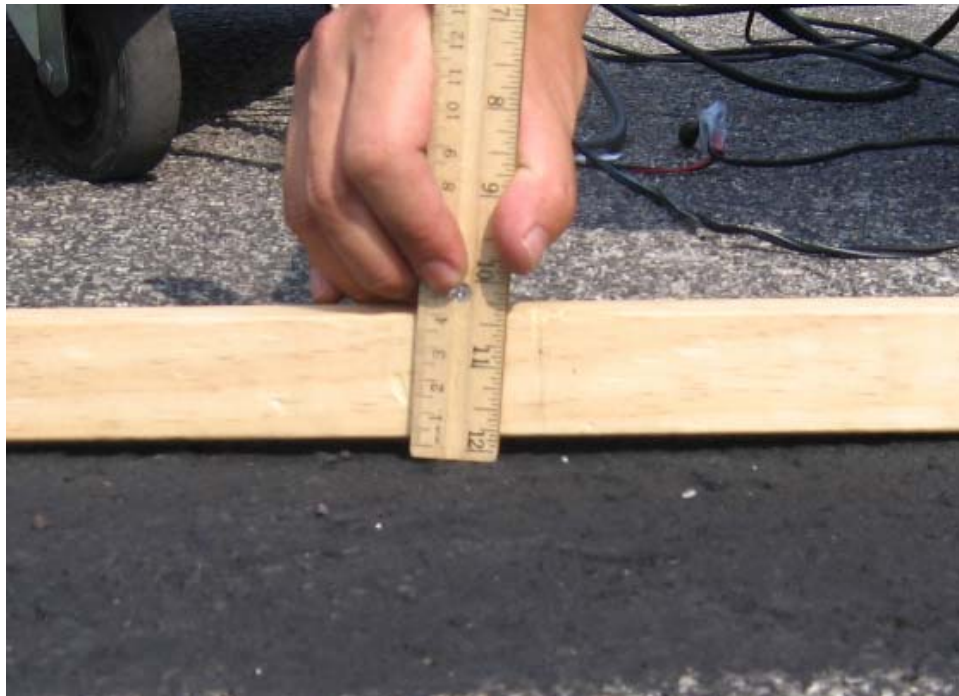


Figure 5.9 The Manual Measurement of the Right Rut Depth

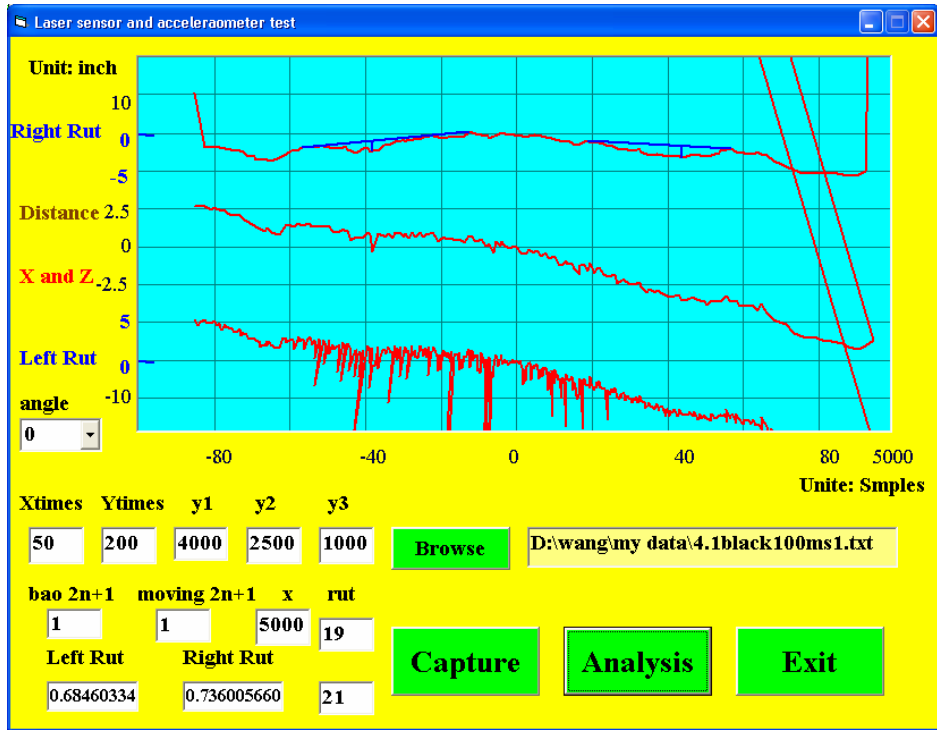


Figure 5.10 On Site Rut Measurement Test 1

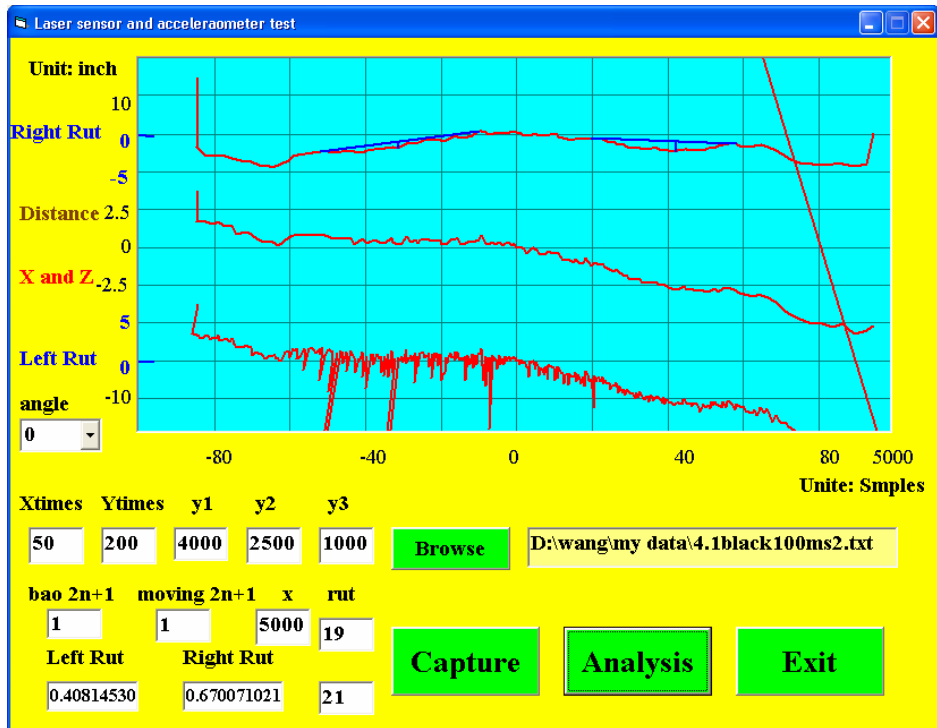


Figure 5.11 On Site Rut Measurement Test 2

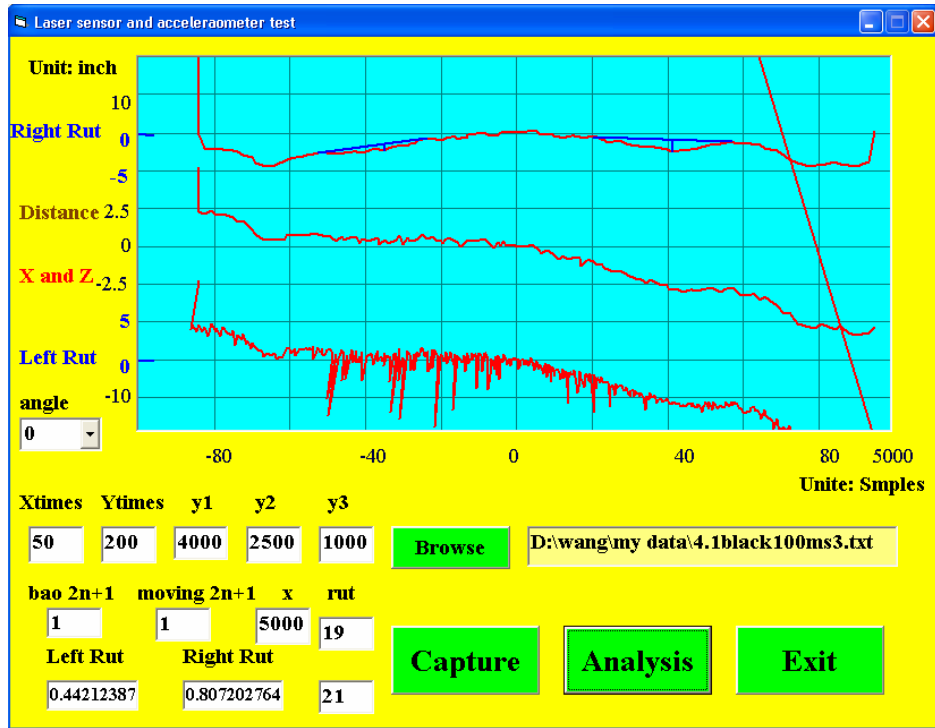


Figure 5.12 On Site Rut Measurement Test 3

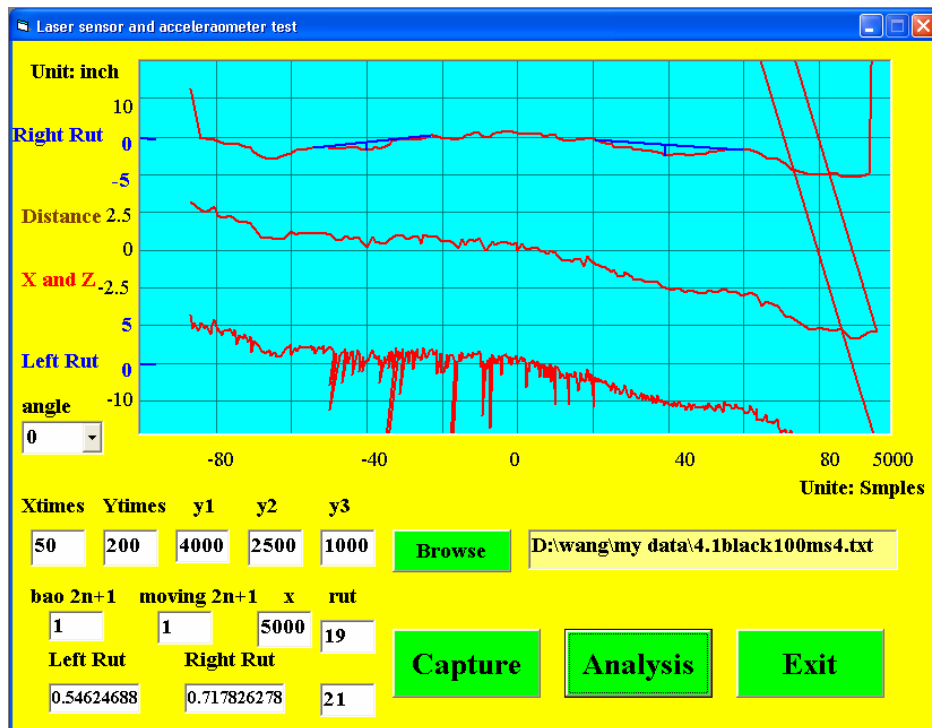


Figure 5.13 On Site Rut Measurement Test 4

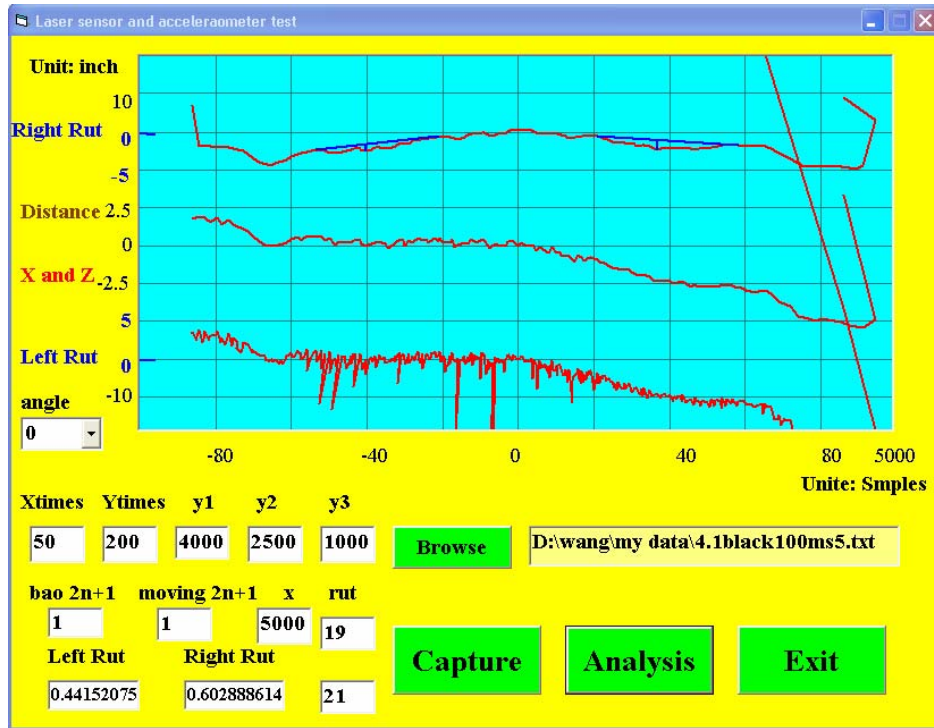


Figure 5.14 On Site Rut Measurement Test 5

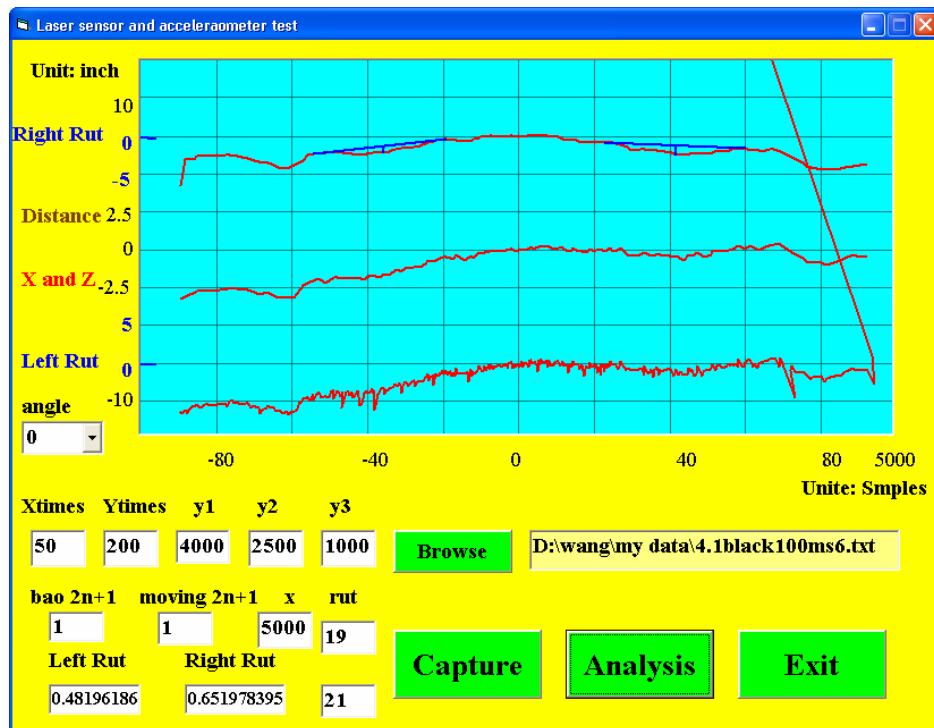


Figure 5.15 On Site Rut Measurement Test 6

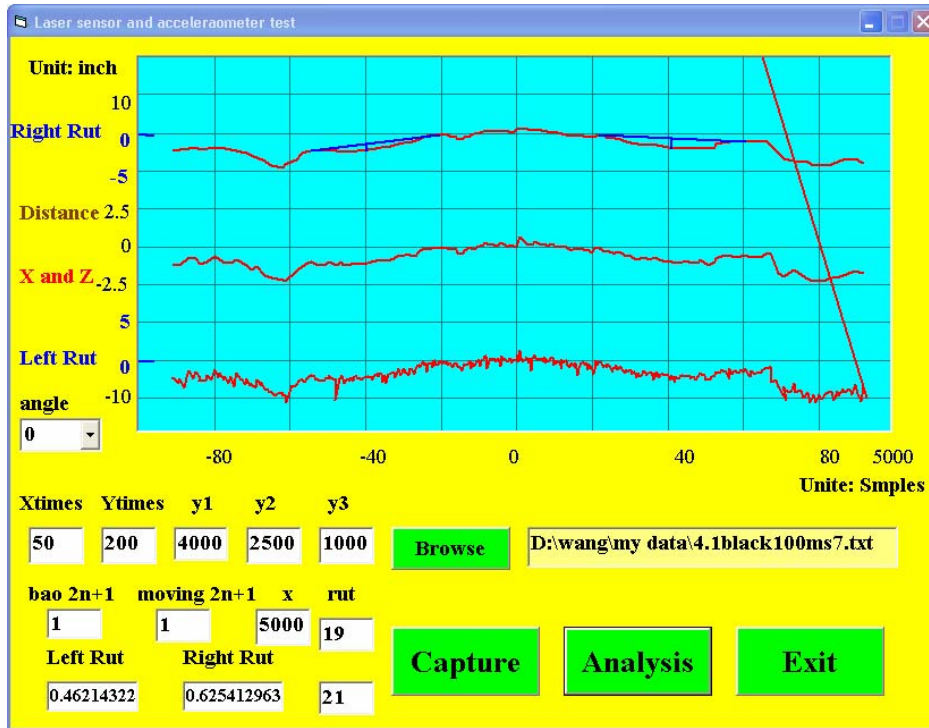


Figure 5.16 On Site Rut Measurement Test 7

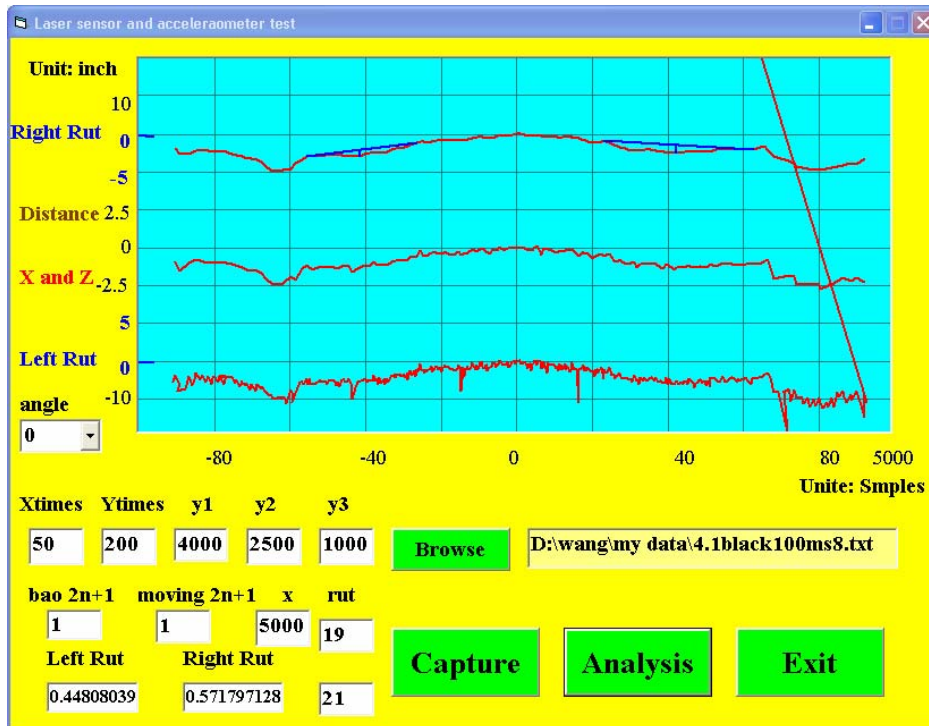


Figure 5.17 On Site Rut Measurement Test 8

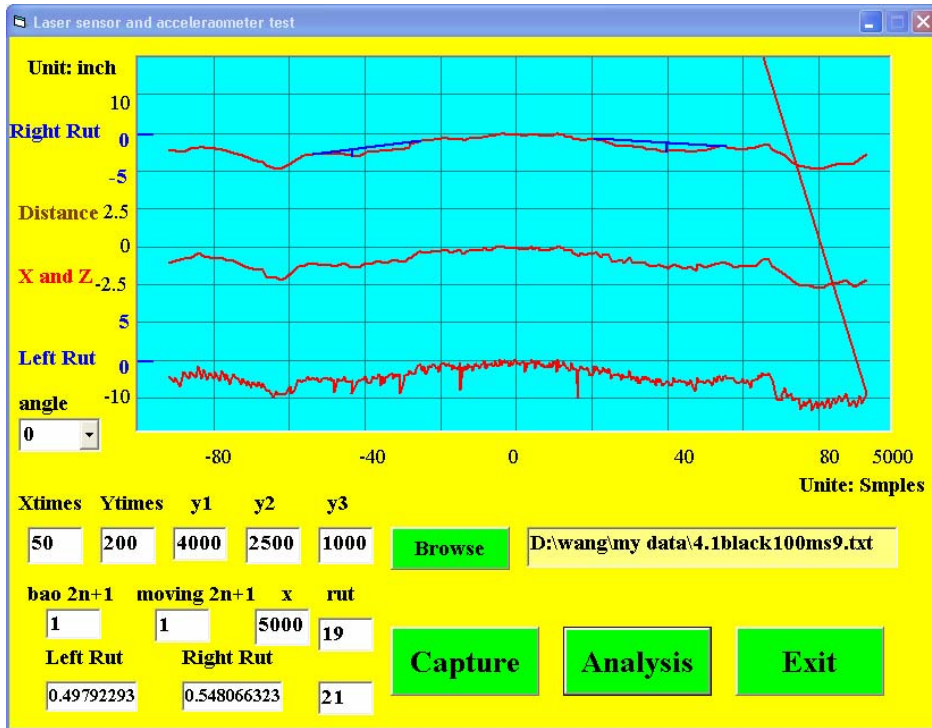


Figure 5.18 On Site Rut Measurement Test 9

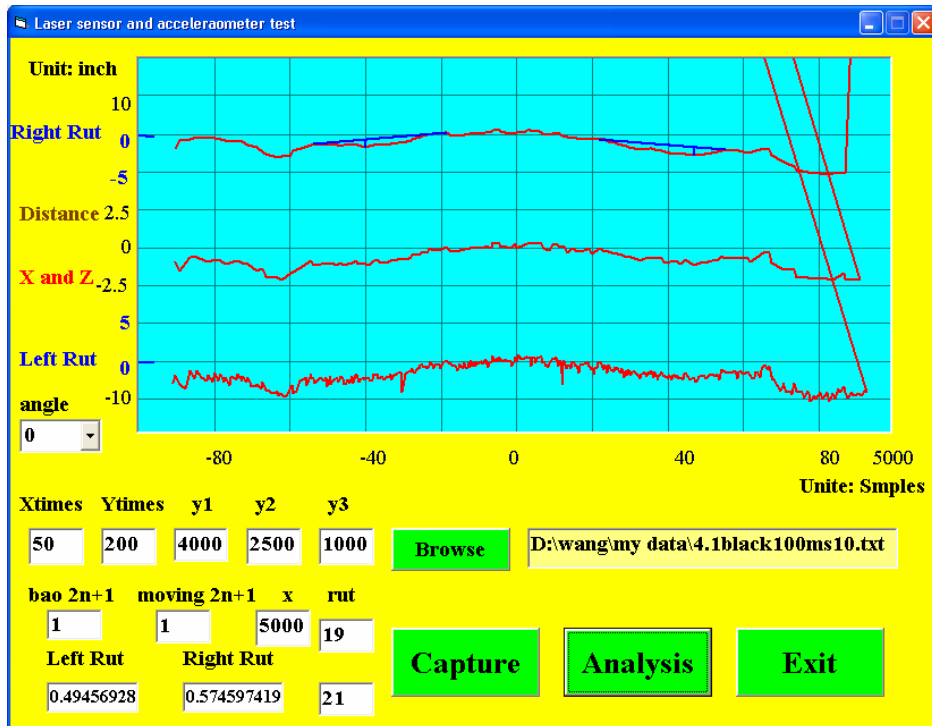


Figure 5.19 On Site Rut Measurement Test 10



Table 5.1 Comparison of Real Rut Depth with 10 Values Obtained by the Scanner

number	left	error	right	error
1	0.685	0.185	0.736	0.086
2	0.408	0.092	0.67	0.02
3	0.442	0.058	0.807	0.157
4	0.546	0.046	0.718	0.068
5	0.442	0.058	0.603	0.047
6	0.482	0.018	0.652	0.002
7	0.46	0.04	0.625	0.025
8	0.448	0.052	0.572	0.078
9	0.497	0.003	0.548	0.102
10	0.495	0.005	0.576	0.074
Real Rut	0.5	$\delta=0.075$	0.65	$\delta=0.079$

From the table, the biggest error was 0.185. The square roots for both left and right rut depths were 0.075 and 0.079 inches respectively. That is to say, the error was less than 2mm. The design capacity enables the relative accurate measurements of rut depth by AR 4000 laser scanner..

## Chapter 6

### SUMMARY, CONCLUSIONS AND RECOMMENDATIONS

#### 6.1 Summary

In the field of transportation, asphalt pavement rutting is one of the most common and destructive pavement distresses on the roads. Rutting problems are most serious in the urban environment at intersections where high volume of traffic is always the case. Rutting is an important indicator of the structural integrity of the pavement and it also has an impact on the safety issues of drivers. For these reasons, it is important to monitor and measure levels of rut depths on the pavement. Until recently, traditional way of rut depth measurement was widely used. It is a manual measurement by ruler in hands. Although the way of measurement is accurate, it had big shortcoming that cannot be overcome without applying new more automated methods. In manual way, only limited data can be obtained which may not be very useful for large scale roads. Recently, several automated technologies are applied in this field. Among them, there are four major technologies used for estimating rut depth in automated measurement way: ultrasonics, point lasers, scanning lasers, and optical. Each method has its advantages and disadvantages. Laser scanning technology excels the other three; however, the cost is also much higher. AR4000 laser scanner was chosen as the laser scanner for this project because of its relatively high power and lower price.

The specifications of AR 4000 provide the basic system requirement. However, some system improvement was conducted by the factory based on the advice from the testing. After the improvement, the AR4000 laser scanner has higher power. A wooden frame was made to hold the scanner which it is working. The test shows favorable results. Software was developed by using the computer language visual basic. The software plays a very important role in the data analysis. Different ways of calibration was also conducted. The laser scanner showed good quality of calibration when the scanner was used to scan flat floor surface and floor with five blocks of different heights.

Real data then were collected by going to the site. When the site was selected, the frame was set up on the site and the laser scanner was running to collect data of the pavement profile. The data sheet in the format of Excel spreadsheet was generated automatically by the built in software of the laser scanner. The collected data were taken by to the office and data analysis was basically conducted in six steps: analysis of data sheets, calculation of initial angles, development of scope line, calculation of moving average, analytical calculation process and the measurement of repeatability and accuracy. These six steps are closely connected with each other. The accomplishment of previous step will eliminate unfavorable factors for the next steps and therefore make the analysis more and more approaching ideal. The software designed by the researcher incorporated many of these steps in the programming. The results of data analysis show that AR4000 can relatively accurately measure the rut depth of the asphalt pavement on the roads. The fact that the same measurement on

the same site for 10 times generating the basically same shaped curves further shows the accuracy of the laser scanner in the real use.

## 6.2 Conclusions

This thesis focused on the development of the laser scanner to effectively measure rut depth. During this process, hardware designed has been improved, computer software has been developed and data collection and data analysis has been conducted.

Evaluation of the accuracy is the big concern of the project. Based on that, correction and improvement of the laser scanner system is realized to strengthen its power, which makes measuring different pavement in different situations possible. That is to say, the capacity of measurement is improved. For the purpose of this project, the researcher paid special attention to the performance measures, more specifically; it is the repeatability and correlativity.

Although the system is not still perfect, and some standard errors still exist, the study did generate some tentative results that may be useful in the field of pavement rutting. From field experiments and data analysis, it shows:

1. Laser scanner showed satisfactory repeatability performances. The repeatability analysis shows that runs of analysis can be reasonably reduced in the later data collection and analysis;
2. Laser scanner has good correlations with manual rut data. The correlation analysis shows that the AR4000 scanner used in the project can be widely used to replace the manual rut measurement; and

3. High power laser scanner has to be used with dark asphalt pavement conditions to lessen the effect of reflectivity of the sun.

### **6.3 Recommendations**

Some recommendations are presented in this section based on the data analysis and project experience. Further research and field experience can be effectively directed by these recommendations.

First of all, the big limitation of this project is that the laser scanner is operating in the still position. Although the results of this measurement can indicate some feature of measurement in a moving vehicle, it is possible that there are some unforeseen factors that will further complicate the measurement process. So it is recommended that the scanner was installed in a moving vehicle to test the rut depth. In this way, it is also to collect large amount of data in a short period of time.

Second, this project confines to use only the laser scanner to measure the rut depth. Optical method is also widely used and generates favorable results. It is recommended that optical methods such as digital camera can be used in the same project and the results from both media can be compared and contrasted.

Last but not least, more research needs to be conducted in the area of rut depth measurement to get more useful data to address the issues in different conditions, such as the correlation between dark asphalt and light pavement, or vice versa.

## REFERENCES

1. Adequacy of Rut Bar Data Collection. Publication No. FHWA-RD-01-027, FHWA Contact: Cheryl Richter, HRDI-13.
2. Bennett, C.R. (2001). Evaluating the Quality of Road Survey Data. Transfund Research Report 200. Transfund New Zealand, Wellington.
3. Bennett, C.R. (1998). Evaluation of a Transverse Profile Logger. Proc. 4<sup>th</sup> International Conference on Managing Pavements, Durban (Available for download from [www.htc.co.nz](http://www.htc.co.nz)).
4. Bennett, C.R. & Paterson, W.D.O., (1999). Guidelines on Calibration and Adaptation. HDM-4 Reference Manual Volume 4. PIARC, Paris.
5. Bennett, C. R. & Wang, H., (2002) Harmonizing Automated Rut Depth Measurements. Data Collection Ltd.
6. Bergh, C. F. & Kennedy, B. A., A Compact, low power two-axis scanning laser rangefinder for mobile robots, Jet Propulsion Laboratory, California Institute of Technology.
7. Cenek, P.D., Patrick, J.E., McGuire, J.F., & Robertson, D.A. (1994). New Zealand Experience in Comparing Manual and Automatic Pavement Condition. Proc. 3rd International Conference on Managing Pavements, San Antonio Vol 2, pp. 265-278.
8. Characterization of Transverse Profiles, Simpson, A.L. Report No. FHWA-RD-01-024, Federal Highway Administration, McLean, Virginia, April, 2001.
9. Darboux, F. & Huang, C., (2003). An Instantaneous-Profile Laser Scanner to Measure Soil Surface Microtopography, Purdue University.
10. Data Collection Ltd. (1996). Accuracy of ROMDAS Ultrasonic Measurement System. Technical Memo ST2. Data Collection Ltd., Auckland (Available for download from [www.ROMDAS.com](http://www.ROMDAS.com)).
11. Hadley, W.O. and Myers, M.G. (1991). Rut Depth Estimates Developed from Cross Profile Data. SHRP Long Term Pavement Performance Program Technical Memo AU-179, Texas Research and Development Foundation, Austin.

12. Herr, B. (2001). Calibration and Operation of Pavement Profile Scanners, Phoenix scientific inc., (Available for download from [http://www.phnx-sci.com/images/pdf/files/2001\\_RPUG\\_PP\\_Movie.ppt](http://www.phnx-sci.com/images/pdf/files/2001_RPUG_PP_Movie.ppt)).
13. HTC (2001b). Validation of ROMDAS Transverse Profile Logger. Internal Report F003/1. HTC Infrastructure Management Ltd., Auckland (available for download from [www.ROMDAS.com](http://www.ROMDAS.com)).
14. Laser Rut Measurement System Developed by INO. (Available for download from [http://www.ino.ca/En/Notre\\_offre/Vision\\_industrielle/realisations/LRMS.aspx](http://www.ino.ca/En/Notre_offre/Vision_industrielle/realisations/LRMS.aspx)
15. Lazic, Z., (2003). Saskatchewan Highways and Transportation, From Road Condition Data Collection to Effective Maintenance Decision Making: Saskatchewan Highways and Transportation Approach.
16. The Nadx Topograph. (Available for download from <http://www.nadx.co.uk/docs/Beam%20Spec.doc>).
17. Reulke, R. & Wehr, A., (2003). High Resolution Mapping Using CCD-line Camera and Laser Scanner with Integrated Position and Orientation System, University of Stuttgart.
18. Simpson, A. (2001). Characterization of Transverse Profiles. Publication FHWARD- 01-024. Federal Highways Administration, McLean, VA. (Available for download from <http://www.tfhrc.gov/pavement/ltp/pdf/01-024a.pdf>).
19. Transfund. (1997). RAMM Road Condition Rating and Roughness Manual. Transfund New Zealand, Wellington.
20. Vedulaet, K. et al., (2002). Comparison of 3-point and 5-point Rut Depth Data Analysis, Kansas State University, Proceedings of the Pavement Evaluation Conference, Roanoke, VA.
21. Willett, M., Magnusson, G., & Ferre, B. (2000). Theoretical Study of Indices. FEHRL Investigation on Longitudinal and Transverse Evenness of Roads— Concluding Workshop, Nantes.